

More About This Article

Additional resources and features associated with this article are available within the HTML version:

- Supporting Information
- Access to high resolution figures



ACS Publications
High quality. High impact.

Journal of Medicinal Chemistry

Subscriber access provided by American Chemical Society

- Links to articles and content related to this article
- Copyright permission to reproduce figures and/or text from this article

[View the Full Text HTML](#)



ACS Publications
High quality. High impact.

Journal of Medicinal Chemistry is published by the American Chemical Society,
1155 Sixteenth Street N.W., Washington, DC 20036

Dihydropyrrole[2,3-*d*]pyridine Derivatives as Novel Corticotropin-Releasing Factor-1 Antagonists: Mapping of the Receptor Binding Pocket by in Silico Docking Studies

Romano Di Fabio,^{*,#} Roberto Arban,[#] Giovanni Bernasconi,[#] Simone Braggio,[#] Frank E. Blaney,[†] Anna M. Capelli,[‡] Emiliano Castiglioni,[#] Daniele Donati,[#] Elettra Fazzolari,[#] Emiliangelo Ratti,[#] Aldo Feriani,[‡] Stefania Contini,[#] Gabriella Gentile,[#] Damiano Ghirlanda,[#] Fabio M. Sabbatini,[#] Daniele Andreotti,[#] Simone Spada,[#] Carla Marchioro,[‡] Angela Worby,[†] and Yves St-Denis[#]

Neurosciences Centre of Excellence for Drug Discovery and Molecular Discovery Research, GlaxoSmithKline Medicines Research Centre, Via A. Fleming 4, 37135, Verona, Italy, and Molecular Discovery Research, GlaxoSmithKline NFSP, Harlow, U.K.

Received June 18, 2008

In an effort to discover novel CRF-1 receptor antagonists exhibiting improved physicochemical properties, a dihydropyrrole[2,3]pyridine scaffold was designed and explored in terms of the SAR of the substitution at the pendent phenyl ring and the nature of the heterocyclic moieties present in the upper region of the molecule. Selective and potent compounds have been discovered endowed with reduced ClogP with respect to compounds known in the literature. Of particular relevance was the finding that the in vitro affinity of the series was maintained by reducing the overall lipophilicity. The results achieved by this exploration enabled the formulation of a novel hypothesis on the nature of the receptor binding pocket of this class of CRF-1 receptor antagonists, making use of in silico docking studies of the putative nonpeptidic antagonist binding site set up in house by homology modeling techniques.

Introduction

Major depression is a complex psychiatric disorder that affects an enormous number of people in society and constitutes a major health concern worldwide. In most cases, major depression is a recurrent lifelong illness, characterized by repeated exacerbation and remission periods. Despite the number of treatments available, mainly addressing the modulation of the monoamine neurotransmitters, significant unmet needs still remain in terms of efficacy, onset of effect, and tolerability. In fact, the current antidepressant drugs take 6–8 weeks to exert their effect and approximately 30% of patients are nonresponders; moreover, drug-induced side effects reduce patient compliance.

Over the past 2 decades extensive research attempts have been made to identify relevant biological targets contributing to the main pathophysiological mechanisms of the anxiety and depressive disorders with the aim of getting more efficacious and safer treatments with rapid symptoms relief. Nowadays, several lines of evidence associate chronic stress with anxiety and depression via the hyperactivation of the hypothalamus–pituitary–adrenal (HPA) axis triggered by the hypersecretion of corticotropin-releasing factor (CRF^a).¹ This neuropeptide, originally isolated by Vale and colleagues² in 1981 from ovine hypothalamus, is considered one of the major biochemical modulators that coordinate the adaptive response of organisms to stress.^{3–6} More

specifically, the acute exposure to adverse stressful conditions is responsible for the production of CRF by parvocellular neurones (PVN) present in the paraventricular hypothalamus; this 41 amino acid neuropeptide is then transported to the anterior pituitary gland, where it stimulates the synthesis of adrenocorticotropin hormone (ACTH),⁷ which in turn triggers the release of glucocorticoids from the adrenal cortex.^{8,9} The latter messengers exert a dual negative feedback regulating the synthesis of CRF in the hypothalamus and the production of ACTH in the pituitary gland, restoring the homeostasis of the HPA axis. However, the sustained activation of these stress-responsive systems could result in a progressive failure to maintain the physiological homeostatic conditions, resulting in an increased susceptibility to develop a variety of psychiatric and stress-related illnesses such as depression and obsessive-compulsive disorders.¹⁰

It is well-known that CRF exerts its biological functions through binding to 2 GPCR subfamily B 7-TM receptors: CRF type-1 (CRF₁) and CRF type-2 (CRF₂) receptor.¹¹

Several lines of clinical evidence suggest the association between hyperdrive of CRF and the onset of anxiety and depressive disorders; namely, (a) high levels of CRF have been found in the CSF of postmortem depressed patients and significant reduction of CRF₁ binding sites in the frontal cortex of suicide victims;¹² (b) increase of CRF mRNA expression has been observed in the hypothalamus of depressive patients;¹³ (c) blunted ACTH response to CRF and abnormal CRF levels are normalized upon clinical recovery after treatment either with fluoxetine^{14,15} or with electroconvulsive shocks;¹⁶ (d) significant reduction of the depression and anxiety scores has been observed in a clinical trial in 20 depressed patients.¹⁷

Following this compelling body of clinical results significant investments have been made in the past 2 decades by several pharmaceutical research groups to discover non-peptide CRF₁ receptor antagonists as a potential treatment for stress-related illnesses including depression. 7*H*-Pyrrolo(2,3-*d*)pyrimidin-4-amine, *N*-butyl-*N*-ethyl-2,5-dimethyl-7-(2,4,6-trimethylphenyl) (CP-154,526),¹⁸ 3-[6-(dimethylamino)-4-methyl-3-pyridinyl]-

* To whom correspondence should be addressed. Phone: +39 045 8218879. Fax: +39 045 8218196. E-mail: rdf26781@gsk.com.s.

[#] Neurosciences Centre of Excellence, GlaxoSmithKline Medicine Research Centre.

[†] Molecular Discovery Research, GlaxoSmithKline Medicines Research Centre, NFSP, Harlow, U.K.

[‡] Molecular Discovery Research, GlaxoSmithKline Medicines Research Centre, Verona, Italy.

^a Abbreviations: CRF, corticotropin-releasing factor; HPA, hypothalamus–pituitary–adrenal; PVN, parvocellular neurons; ACTH, adrenocorticotropin hormone; GPCR, G-protein-coupled receptor; CSF, cerebrospinal fluid; TM, transmembrane; PLS, partial least squares; PSA, polar surface area; PCA, principal component analysis; VIP, variable importance; RMSEE, root mean square error of estimation; SDM, site direct mutagenesis; SAR, structure–activity relationship; QSAR, quantitative structure–activity relationship.

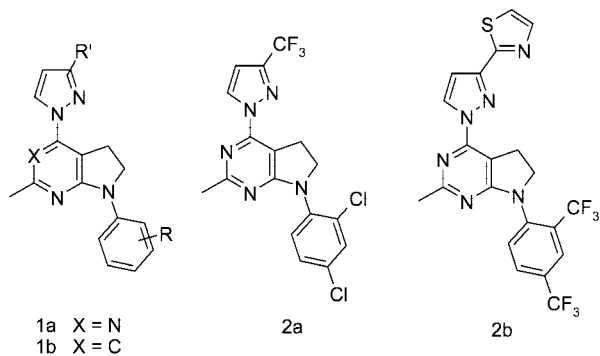


Figure 1. Exploration of the pyrrolidinepyridine template.

2,5-dimethyl-*N,N*-dipropylpyrazolo[1,5-*a*]pyrimidin-7-amine (R121919),¹⁸ and **3** (DMP-696)¹⁸ are among the first and the most representative compounds identified. These CRF-1 antagonists exhibited both high *in vitro* affinity and receptor selectivity coupled with a significant *in vivo* activity in animal models of anxiety. More recently, a variety of alternative classes of monocyclic, bicyclic, and tricyclic derivatives have been disclosed, thus further broadening the structural diversity and the knowledge of the structure–activity relationship (SAR) for the CRF-1 antagonists binding site.¹⁸ Notwithstanding the significant progresses made in the latter respect, to date, very few molecules have reached an advanced preclinical development and/or clinical phases mainly because of the lack of the required druglike properties. More specifically, most of the compounds identified were highly lipophilic and hence associated with unsuitable pharmacokinetics and toxicological profile.¹⁸

As part of a broad chemical strategy aimed toward the discovery of novel CRF-1 antagonists, we designed and explored the dihydropyrrole[2,3-*d*]pyrimidine template of type **1a** shown in Figure 1. In particular, after the identification of the central core of the molecule we identified an appropriate decoration of the upper region of the molecule to reduce the general lipophilicity, thus improving the metabolic stability and the overall developability profile.^{19,20} This strategy diverges significantly from the known SAR available in literature, namely, the common belief that flexible/long acyclic carbon chains were necessary to maximize the *in vitro* affinity at the CRF-1 binding site. Compounds **2a** and **2b** (Figure 1) were identified as the most interesting derivatives belonging to this new series. Notably, these compounds exhibited good *in vitro* affinity and excellent pharmacokinetics in rat.²¹

To optimize further their general physicochemical properties, thus improving their druggability, we decided to replace the dihydropyrrole[2,3-*d*]pyrimidine core of type **1a** with the corresponding dihydropyrrole[2,3-*d*]pyridines **1b** with the specific aim to fine-tune the basicity of the aromatic nitrogen. Meanwhile, to reduce the overall lipophilicity, we managed to expand the exploration of both the substitution at the pendent phenyl ring and the nature of the heterocyclic moieties present in the upper region of the molecule. Further novel hypotheses on the nature of the receptor binding pocket of this class of CRF-1 receptor antagonists have been postulated by *in silico* docking studies of the putative nonpeptidic antagonist binding site set up in house by homology modeling techniques.

Chemistry

Compounds **4–39** were prepared following the general synthetic procedure shown in Scheme 1. The starting compound **47**, obtained as previously reported,²² was transformed into **48**

by chemoselective nucleophilic aromatic substitution with appropriate substituted pyrazoles, reaction occurring in good chemical yield at the less hindered C-4 position. The following reduction of the ester function by DIBAL-H in CH₂Cl₂, followed by oxidation by Dess–Martin's reagent, enabled the preparation of aldehyde derivatives of type **50**, which were efficiently elongated to give the corresponding analogues **51**. Then the sequential reduction of the aldehyde group to primary alcohol followed by protection as TBS afforded intermediates **53**, which were transformed into **54** by a Buchwald-type reaction in the presence of different substituted aniline and/or pyridine derivatives. Finally, removal of the TBS protecting group followed by the transformation of the primary alcohol into the corresponding mesylate, iodide, or bromide derivatives gave rise to spontaneous cyclization to afford the desired title compounds **4–39**.

As far as the obtaining of compounds **40** and **41** is concerned, as shown in Scheme 2, intermediate **50** was transformed into **56** by Wittig-type reaction followed by Buchwald-type coupling reaction with 2-methyl-4-methoxyaniline mediated by microwave irradiation. Then the hydrolysis of the enolate function led to the final indole derivative **40** in good total chemical yield. Alternatively, when compound **50** was treated with hydrazine monohydrate and the solution irradiated in a microwave apparatus for 10 min, bicyclic derivative **57** was obtained in 54% yield after purification by flash chromatography. This intermediate was then reacted with 3-methyl-4-bromobenzonitrile according to Buchwald's reaction conditions to yield the title compound **41**, although in poor chemical yield.

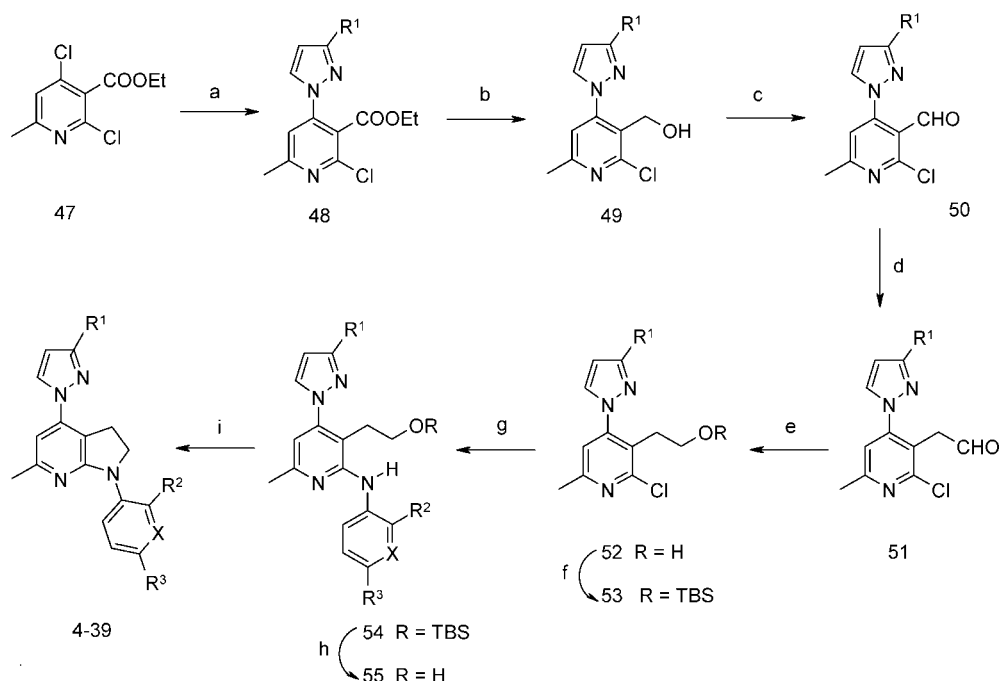
Compounds **42–44** were synthesized, as shown in Scheme 3, from commercially available intermediate **58**. Reaction with POCl₃ followed by chemoselective aromatic nucleophilic substitution at the C-4 position afforded nitro derivative **60**, which then was transformed into **61** by the usual Buchwald-type reaction, this time in the presence of 2,4-bis(trifluoromethyl)aniline. Reduction of the nitro group gave the corresponding amine derivative **62**, which was then transformed into final compound **42** in 50% yield by reaction with triphosgene in the presence of triethylamine. Alternatively, final compounds **43** and **44** were prepared in quantitative yield from the common intermediate **62** by reaction with a 1:1 mixture of acetic acid/acetic anhydride at 90 °C for 2 h and trifluoroacetic acid/trifluoroacetic anhydride at reflux for 2 h, respectively.

Compound **45** was synthesized in six steps from intermediate **49** as shown in Scheme 4. The sequential protection of the primary alcohol, Buchwald-type reaction with 2,4-bis(trifluoromethyl)aniline and deblocking of the TBS, afforded intermediate **65**, which was transformed into the key primary chloride derivative **66**. Reaction with Na₂SO₃ in CH₃CN at room temperature afforded the sulfonic acid intermediate **67** in quantitative yield, which was transformed into the final compound **45** in 49% yield by reaction with POCl₃ at 170 °C for 20 min.

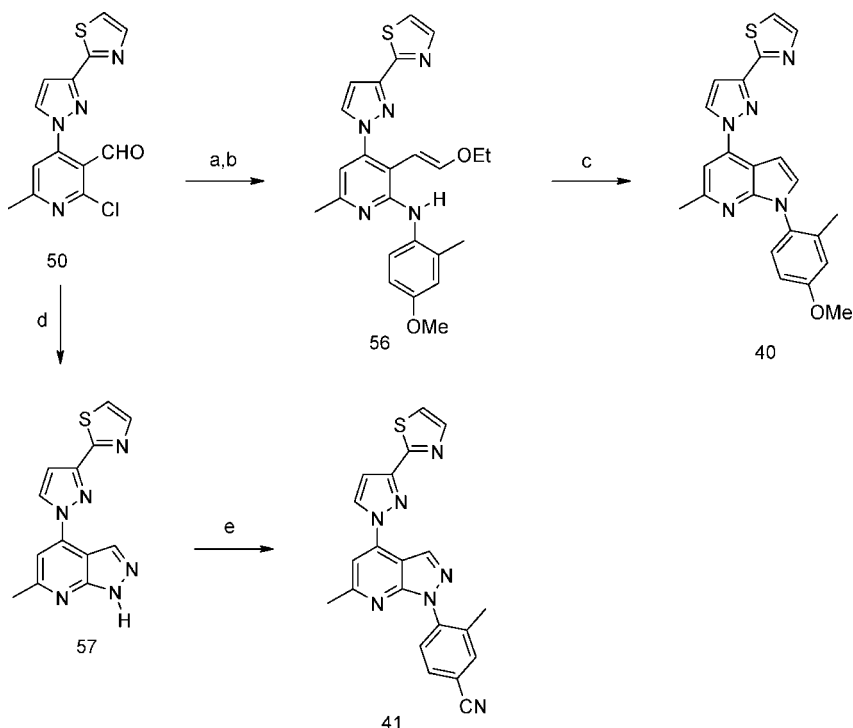
Compound **46** was prepared in three steps, as shown in Scheme 5, from the commercially available starting material **68**. The key reaction was, once again, the Buchwald-type aromatic substitution reaction between intermediate **70** and 5-methoxy indoline **71**, with a 19% chemical yield after microwave irradiation.

Results

The initial exploration performed was aimed at clarifying whether the dihydropyrrole[2,3-*d*]pyrimidine core could have been replaced by the corresponding dihydropyrrole[2,3-*d*]py-

Scheme 1. General Synthetic Procedures for the Preparation of Compounds 4–39^a

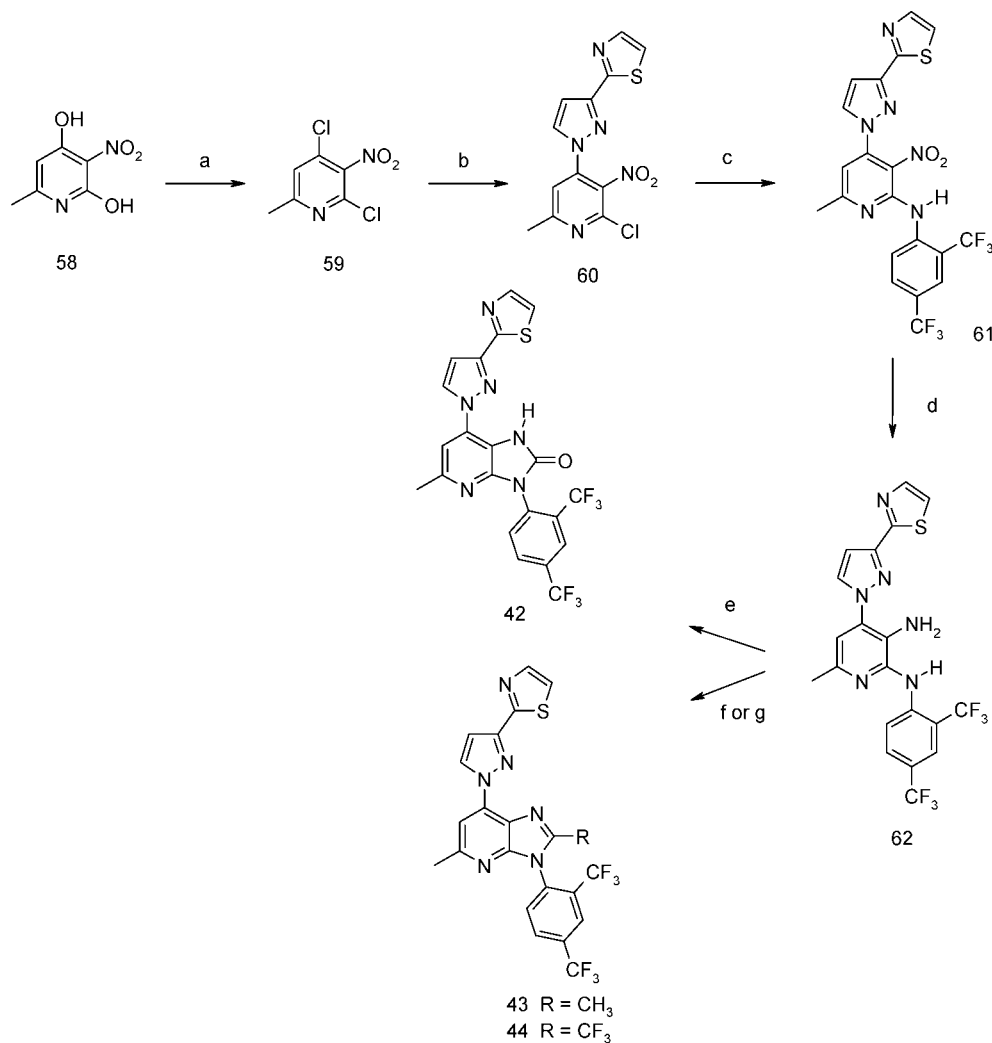
^a Reagents and conditions: (a) 3-substituted pyrazole, NaH, DMF, 0 °C, 10 min, room temp 1 h, then **47** $T = 110$ °C, 3 h; (b) DIBAL-H (1 M) in hexanes, CH_2Cl_2 , -78 °C to room temp, 2 h; (c) Dess–Martin's reagent, CH_2Cl_2 , room temp, 1 h; (d) (i) $\text{Ph}_3\text{PCH}_2\text{OMe}$, 1.6 M *n*-BuLi in hexanes, THF, $T = 0$ °C to room temp, 15 min, then addition of **50**, room temp, 1.5 h; (ii) 6 N HCl, THF, room temp, 15 h; (e) CeCl_3 , NaBH_4 , MeOH, room temp, 5 min; (f) 2,6-lutidine, TBSOTf, CH_2Cl_2 , room temp, 15 h; (g) $\text{Pd}_2(\text{dba})_3$, 2-(dicyclohexylphosphino)-2'-methylbiphenyl, DME, K_3PO_4 , ArNH_2 , microwave irradiation, $T = 100$ °C, 20 min; (h) $\text{Et}_3\text{N}\cdot 3\text{HF}$, THF, room temp, 15 h; (i) MsCl , Et_3N , DMF, 56 °C, 4 h or I_2 , PPh_3 , Et_3N , CH_2Cl_2 , room temp, 2 h or CBr_4 , PPh_3 , Et_3N , CH_2Cl_2 , room temp, 2 h.

Scheme 2. General Synthetic Procedures for the Preparation of Compounds 40 and 41^a

^a Reagents and conditions: (a) $\text{Ph}_3\text{PCH}_2\text{OMe}$, 1.6 M *n*-BuLi in hexanes, THF, $T = 0$ °C to room temp, 15 min, then addition of **50**, room temp, 1.5 h; (b) $\text{Pd}_2(\text{dba})_3$, 2-(dicyclohexylphosphino)-2'-methylbiphenyl, K_3PO_4 , 2-Me-4-OMe-aniline, microwave irradiation, 100 °C, 10 min; (c) 6 N HCl, THF, room temp, 15 h; (d) $\text{NH}_2\text{NH}_2\cdot \text{H}_2\text{O}$, EtOH, microwave irradiation, $T = 100$ °C, 10 min; (e) 4-Br-3-Me-benzonitrile, Cs_2CO_3 , CuI, 1,2-cyclohexanediamine, dioxane, $T = 140$ °C, 2 h.

ridine template analogue. To this end, the bis- CF_3 derivative **4** was prepared as described above and characterized in terms of the in vitro affinity to the CRF-1 receptor binding site. As shown

in Table 1, this compound exhibited similar in vitro potency as compound **3** ($\text{pIC}_{50} = 7.56$ and 7.50, respectively).²⁰ Further to this encouraging result, a careful selection of the substituents

Scheme 3. General Synthetic Procedures for the Preparation of Compounds **42–44**^a

^a Reagents and conditions: (a) POCl₃, reflux, 3h. (b) 2-(1H-pyrazol-3-yl)-1,3-thiazole, NaH, DMF, room temp, 20 min, then **59**, room temp, 90 min; (c) Pd₂(dba)₃, dicyclohexyl(2'-methyl-2-biphenyl), K₃PO₄, 2,4-bis(trifluoromethyl)aniline, microwave irradiation, DME, T = 100 °C, 20 min; (d) Na₂S₂O₃, MeCN, room temp, 90 min; (e) triphosgene, Et₃N, THF, room temp, 3 h; (f) AcOH/Ac₂O 1:1, 90 °C, 2 h; (g) TFA/Tf₂O 1:1, reflux, 2 h.

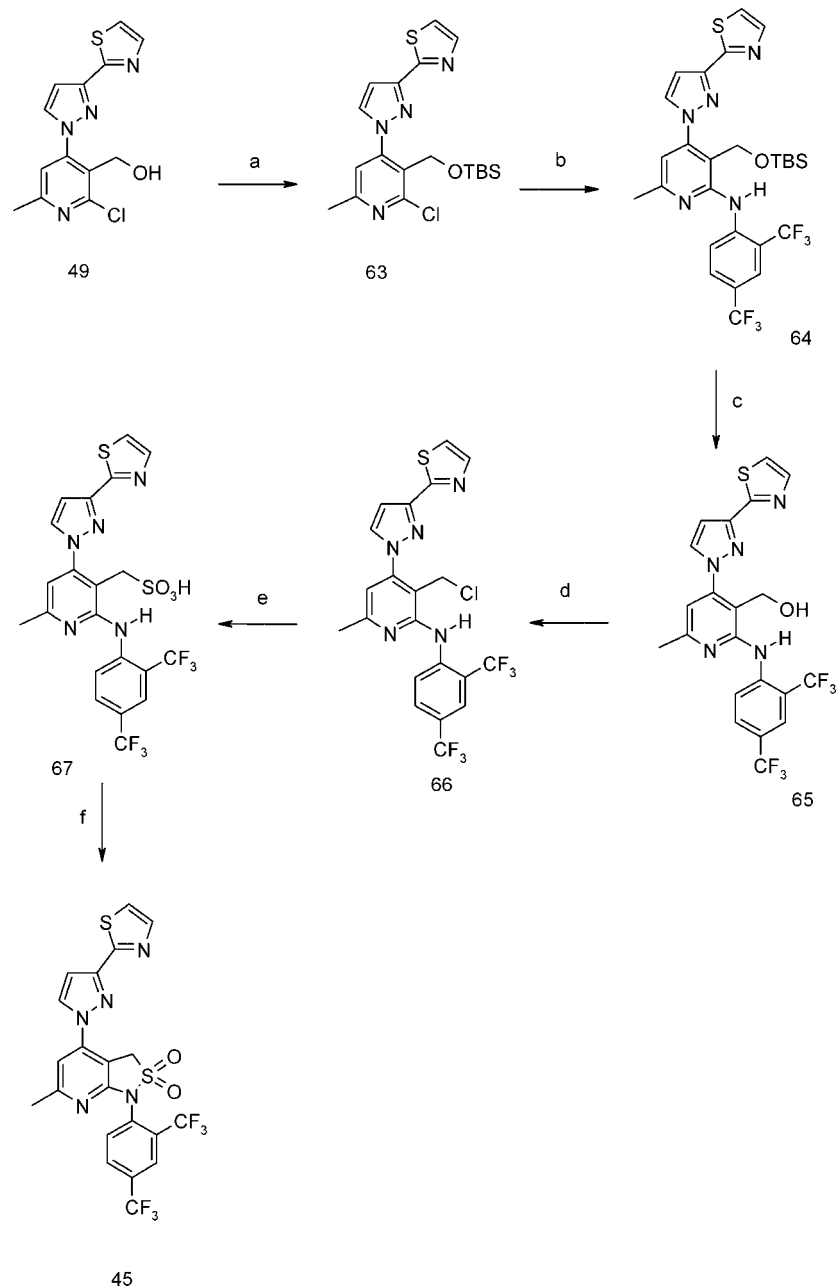
of the pendent phenyl ring was made to clarify further the effects of the substituents, reducing meanwhile the overall lipophilicity, which was too high for compound **4** (ClogP = 6.84). To this end, the series of substituted dihydropyrrole[2,3-*d*]pyridine derivatives **5–33** shown in Table 1 was prepared. Among those, compounds **27** and **32** exhibited the highest in vitro affinities (pIC₅₀ = 7.46 and 7.40, respectively) and reduced ClogP values with respect to compound **4** (clogP = 5.13 and 5.36, respectively). Notably, the presence of an appropriate ortho substituent looks important to increase the in vitro potency; in fact, the corresponding monosubstituted compound **28** (R' = H, R'' = OMe) was in found to be less active (pIC₅₀ = 5.06).

As far as the substitution of the para position of the pendent phenyl ring is concerned, most of the substituents introduced were tolerated, with the only exception of compounds **11** and **12**, whose lower activity was explained by the H-bond donor nature of the hydroxy moiety, most likely detrimental for the activity, and the high steric bulk of the 3,5-disubstituted isoxazole group, respectively.

The replacement of the 2-thiazole ring by a 2-pyridine or a 1-pyrazole in the upper region of the molecule was tolerated. In particular, as shown in Table 1, the 2-pyridyl derivative **36** exhibited similar in vitro activity compared to the corresponding 2-thiazole derivative **6** (pIC₅₀ = 7.03 and 7.06, respectively),

whereas the pyrazole analogue **39** was still active (pIC₅₀ = 6.84), emphasizing the need for the presence of an appropriate H-bond acceptor group in this region of the molecule.

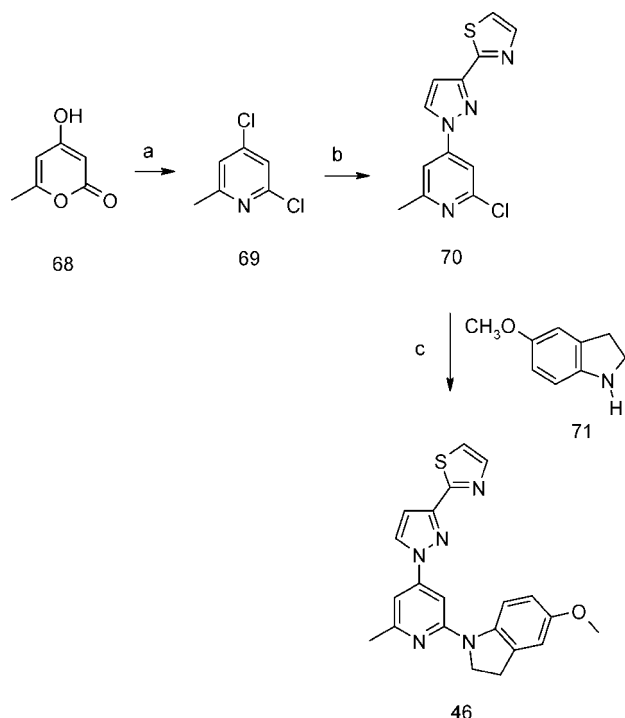
After this exploration, several modifications of the bicycle core of the molecules were also attempted to further clarify the SAR of this series of molecules. To this end, compounds **40–46** shown in Figure 2 were prepared. As shown in Table 1, the indole derivative **40** exhibited a partial reduction of the in vitro potency with respect to the corresponding pyrrolidine analogue **7** (pIC₅₀ = 6.37 and 7.27, respectively), while the introduction of an extra nitrogen atom seems to be responsible for a significant drop of potency (pIC₅₀ = 5.56 and 7.00 for compound **41** and **8**, respectively). Additional modifications introduced in the five-membered core ring in terms of both increased polarity (compounds **42** and **45**) and steric bulk (compound **43** and **44**) made these compounds significantly less active. Finally, a different arrangement of the same structural motifs present in the pyridopyrrolidine derivatives was not tolerated (see compound **46**), confirming the importance of adopting a favorable conformation for the activity in which the pendent phenyl ring is perpendicular to the plane of the dihydropyrrole[2,3-*d*]pyridine core.

Scheme 4. General Synthetic Procedures for the Preparation of Compounds **45**^a

^a Reagents and conditions: (a) TBSCl, Imidazole, DMAP, DMF, room temp, 12 h; (b) Pd₂(dba)₃, 2-(dicyclohexylphosphino)-2'-methylbiphenyl, K₃PO₄, 2,4-bis(trifluoromethyl)aniline, microwave irradiation, DME, *T* = 100 °C, 20 min; (c) Et₃N·3HF, THF, room temp, 15 h; (d) SOCl₂, 40 °C, 1 h; (e) Na₂SO₃, MeCN, room temp, 15 min; (f) POCl₃, *T* = 170 °C, 20 min.

Partial Least-Squares Projection to Latent Structures (PLS):^{23–28} Modeling of the Potency. To identify the relevant physicochemical substituent parameters determining *in vitro* activity at the CRF1 receptor antagonists binding site, a QSAR analysis of the potency (pIC₅₀) was performed using a panel of Hansch classical descriptors for the aromatic substituents,²⁹ in addition to other easily derived properties, namely, PSA and H donors and acceptors (see Table A in Supporting Information), to describe the R₂ and R₃ variation of the compounds shown in Table 1. Both a dummy and the difference in ClogP (Dy_{lip}) variables were used to account for the presence of a 3-pyridyl group as pendent aromatic ring (compounds **30–33**), while differences in ClogP and PSA (ClogP-north and PSA-north) were also included to model the replacement of the 2-thiazole moiety present in the upper region of the molecule by a

2-pyridine or 1-pyrazole ring (compounds **34–39**). Finally, a few classical whole molecule properties (count of features, ClogP, PSA, MW) were added to complete the compound description. For the statistical analysis, a multivariate regression approach (partial least-squares projection to latent structures, PLS), implemented in the SIMCA-P+11.5³⁰ package, was used. Initially, only compounds exhibiting both pIC₅₀ > 5 and the necessary parameters available for the complete description of R₂ and R₃ substituents were considered. Accordingly, compounds **9**, **12**, **22–25**, and **27** were excluded. PCA (principal component analysis) on independent variable (*X*) was run resulting in the identification of a major structural outlier **26**, which was also removed. PLS was hence applied on the 28 remaining compounds, and statistically meaningful models were derived by the Krzanowski cross-validation procedure.³¹ How-

Scheme 5. General Synthetic Procedures for the Preparation of Compounds **46**^a

^a Reagents and conditions: (a) (i) NH_4OH , EtOH, $T = 130^\circ\text{C}$, 24 h; (ii) POCl_3 , $T = 120^\circ\text{C}$, 36 h; (b) (i) 2-thiazole-3-pyrazole, NaH, DMF, room temp, 20 min; (ii) **71**, DME, $T = 100^\circ\text{C}$, 2.5 h; (c) $\text{Pd}_2(\text{dba})_3$, 2-(dicyclohexylphosphino)-2'-methylbiphenyl, DME, K_3PO_4 , microwave irradiation, $T = 100^\circ\text{C}$, 10 min (8 cycles).

ever, none of them were able to predict the lower activity of compounds **22**–**25**, most likely because of the relatively low spread present in the R_2 and R_3 substituent descriptors and the limited range in the independent variable used in the analysis. We hence included compounds with $\text{pIC}_{50} < 5$, setting for them an arbitrary value of 4.5, not too far from the minimum measured value (compound **28**, $\text{pIC}_{50} = 5.06$), in order to avoid a too high distortion in the data structure. This approach was pursued because we are interested in developing understanding and interpretation of the results rather than purely for predictive purposes. A two-component PLS model was then derived (M1), explaining 83% (R^2) of the overall variability in the pIC_{50} values with a cross-validated Q^2 of 76% and $\text{RMSEE} = 0.40$. Removal of the outlier compound **11**, with a predicted activity beyond 2 RMSEE with respect to the observed value, improved substantially the quality of the model ($R^2 = 86.8\%$, $Q^2 = 79.9\%$, $\text{RMSEE} = 0.35$, model M2). Only the activity of compound **20** is overestimated probably because of the size of the substituent present in the ortho position (2-thiophene). Feature selection was carried out using SIMCA VIP (variable importance) and coefficient plots with the objective of creating a “parsimonious”, easy to be interpreted model. The contribution of the original variables to the model components is shown in the loading plot as depicted in Figure 3.

Converting the latent variables t to the native variables, a QSAR equation (MLR-like eq 1) was obtained whose coefficients are summarized in Table 2 while the scaled and centered coefficients are showed in Figure 4, along with the standard deviations determined by bootstrap analysis.

$$\text{pIC}_{50} = 0.44\text{PI}(\text{Ar})_o + 1.23\text{Ver_B2}_o - 0.51\text{SL_F}_o - 0.02\text{PSAo} - 0.41\text{Acc_p} + 4.4 \quad (1)$$

Table 1. Top and Bottom Region SAR

The chemical structure shows a pyridine ring substituted at the 2-position with a thiazole ring (substituted with R^1), at the 3-position with a pyrazole ring (substituted with R^2), and at the 4-position with a benzene ring (substituted with R^3 and X).

compd	R^1	R^2	R^3	X	pIC_{50}^a
3					7.40 ± 0.06
4	2-thiazole	CF_3	CF_3	C	7.56 ± 0.24
5	2-thiazole	CF_3	NO_2	C	7.23 ± 0.21
6	2-thiazole	CF_3	CN	C	7.06 ± 0.04
7	2-thiazole	CH_3	OCH_3	C	7.27 ± 0.18
8	2-thiazole	CH_3	CN	C	7.00 ± 0.16
9	2-thiazole	CH_3	1-pyrazole	C	6.89 ± 0.26
10	2-thiazole	CH_3	F	C	6.79 ± 0.02
11	2-thiazole	CH_3	OH	C	5.46 ± 0.01
12	2-thiazole	CH_3	3,5-dimethyl-2-isoxazole	C	< 5
13	2-thiazole	CH_3	OCF_3	C	6.59 ± 0.13
14	2-thiazole	CH_2CH_3	CN	C	6.90 ± 0.21
15	2-thiazole	OCH_3	OCH_3	C	6.76 ± 0.06
16	2-thiazole	OCF_3	CN	C	6.80 ± 0.17
17	2-thiazole	Cl	OCH_3	C	7.25 ± 0.06
18	2-thiazole	Cl	CN	C	6.64 ± 0.03
19	2-thiazole	Cl	SO_2CH_3	C	5.63 ± 0.10
20	2-thiazole	2-thiophene	CN	C	6.07 ± 0.09
21	2-thiazole	CN	CN	C	5.13 ± 0.21
22	2-thiazole	NO_2	F	C	< 5
23	2-thiazole	NO_2	Cl	C	< 5
24	2-thiazole	NO_2	CN	C	< 5
25	2-thiazole	NO_2	OCH_3	C	< 5
26	2-thiazole	SO_2CH_3	SO_2CH_3	C	5.41 ± 0.21
27	2-thiazole	CHF_2	OCH_3	C	7.46 ± 0.15
28	2-thiazole	H	OCH_3	C	5.06 ± 0.01
29	2-thiazole	F	CN	C	5.69 ± 0.06
30	2-thiazole	CH_3	OCH_3	N	7.22 ± 0.24
31	2-thiazole	OCH_3	OCH_3	N	6.67 ± 0.09
32	2-thiazole	CF_3	OCH_3	N	7.40 ± 0.21
33	2-thiazole	CH_3	$\text{N}(\text{CH}_3)_2$	N	6.59 ± 0.10
34	2-pyridine	Cl	CN	C	6.44 ± 0.14
35	2-pyridine	CH_3	CN	C	6.65 ± 0.14
36	2-pyridine	CF_3	CN	C	7.03 ± 0.07
37	1-pyrazole	CH_3	CN	C	6.50 ± 0.05
38	1-pyrazole	Cl	CN	C	6.94 ± 0.20
39	1-pyrazole	CF_3	CN	C	6.84 ± 0.10
40					6.37 ± 0.10
41					5.56 ± 0.06
42					5.08 ± 0.03
43					< 5
44					< 5
45					< 5
46					< 5

^a Mean $\text{pIC}_{50} \pm \text{SEM}$, h-CRF₁.

$n = 31$, $A = 2$, $\text{RMSEE} = 0.35$, $R^2 = 0.87$, $Q^2 = 0.80$ where n , A , RMSEE , R^2 , and Q^2 are the number of compounds, the number of components, the root mean square error of estimation, the conventional correlation coefficient, and the cross-validated r^2 value (Krzyszowski³¹), respectively (Table 3).

The pIC_{50} values calculated by equation 1 are shown in Figure 5. The model (M2) allows a correct prediction of the activity of compound **9**, previously excluded (see above) as the native variable for the para substituent. The count of H-bond acceptors (Acc_p) is available. Compound **12**, which could have been included for the same reason, was shown to be a structural outlier for the relative large size of the substituent present in the para position.

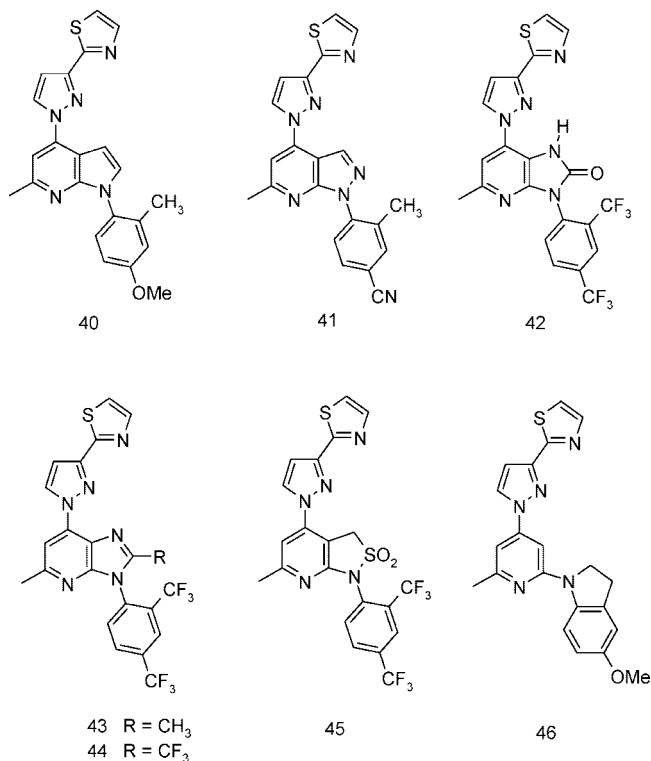


Figure 2. Exploration of the core of the molecule.

According to the coefficients of the native variables, the following conclusions can be drawn for the substituent in ortho position: (a) the *in vitro* activity increases by increasing the lipophilicity and decreasing the polar surface area; (b) the shape descriptor of the ortho substituent (Ver_B2) plays an important role that could be attributed either to a direct effect (shape complementarity to the binding site) or to an indirect effect; i.e., this substituent forces the dihedral angle between the bicycle core and the pendent aromatic ring to adopt a favorable conformation for the activity; (c) an electron donor group in the ortho position (inductive effect, SL_Fo) increases the *in vitro* activity.

The effect in the para position is less clear, as the only descriptor important in the model is the number of H acceptors, which may account for the presence of polar atoms in the para substituent. Furthermore, this is mostly a two-level variable (0/1) and hence poorly discriminant. Finally, the higher activity predicted for the model outlier compound **11** might be explained by the presence of a hydrogen donor group; however, it is worth emphasizing that this compound is unique in the data set.

On the basis of this set of results, the para substituent should lie in a nonpolar pocket with a limited size.

In Silico Docking Studies. To firm up the structural hypothesis expressed above and to further clarify the role of the 2-thiazole moiety present in the upper region of the molecule and/or the corresponding 2-pyridyl or the 1-pyrazole moieties as H-bond acceptor groups, docking studies of compound **7** in the putative nonpeptidic antagonist binding site were performed using an *in silico* model of CRF-1 receptor set up in house by homology modeling techniques.

The model of the CRF-1 receptor was based on previously constructed models of the calcitonin and glucagon receptors, which are both members of the family B proteins. Although it is often quoted that there is no sequence identity between family A and family B 7TM receptors, both families have a number of amino acid residue motifs in common. These include the

cysteine at the top of TM3, a tryptophan in TM4, a proline in TM6, and an asparagine in TM7. Furthermore, the familiar DRY motif in TM3 of family A receptors is replaced by an EXXY quartet at the equivalent position in family B. By use of the crystal structure of rhodopsin³² as a template and sequence alignments of TM3, TM4, TM6, and TM7 based on the conserved motifs mentioned above, an initial model was built of these four helices. For the remaining helices, Fourier analyses of their multiple sequence alignments³³ identified the probable inward facing residues. A series of site directed mutagenesis studies previously carried out on the glucagon and calcitonin receptors had established that some basic lysine, arginine, and histidine residues on the cytoplasmic side of TM2 and TM6 were involved in the activation of family B 7TM and that they were likely to be interacting with the conserved TM3 and TM7 glutamic acids. These were used as additional interhelical constraints for placement of the remaining three helices. The resulting models of these two receptors were used as templates for the construction of the CRF-1 protein. The starting structure was fully minimized using the CHARMM program,³⁴ with 500 steps of steepest descent and 5000 steps of ABNR, using a constant dielectric of 5 to reduce the overwhelming effects of the electrostatic contribution at this stage. NOE distance constraints were applied to the helical backbone hydrogen bonds (a range of 1.8–2.4 Å was used for the distance between the *i*th residue's backbone carbonyl and the (*i* + 4)th residue's amide hydrogen). Proline residues of course had no restraint. Prior to minimization, side chain conformations were set to those described in the rotamer library of Karplus and Dunbrack³⁵ using the Protein Design module within the Quanta program. They were not, however, further constrained during the minimization. The interhelical constraints described above were applied by simply fixing the positions of the TM2 arginine and histidine, the TM3 glutamate, the TM6 lysines, and the conserved TM7 glutamate, which is proposed to form an "ionic lock" with the adjacent lysine on TM6. There was not much deviation between the models before and after minimization, with the exception of TM4 which had generally shifted toward the extracellular side with C α deviations of up to 3.3 Å. However, in the docking described below, TM4 does not contribute to the binding pocket.

The CRF-1 receptor antagonist **7** was docked in the nonpeptidic antagonist binding site of the CRF1 receptor model. Flexible docking experiments were carried out by performing Monte Carlo sampling coupled with energy minimization of the sampled complexes with AMBER united atom force field implemented in MacroModel/Batchmin routines.³⁶ The numbering system of the amino acid receptors is consistent with that published in the literature.³⁷ As can be seen in Figure 6A, in the energetically favorable docking solutions obtained for compound **7**, the pyridine core nitrogen adjacent to the pendent phenyl ring acts as H-bond acceptor interacting with His199 in the third transmembrane domain, while the core ring structure is close to Met276 in the fifth transmembrane domain. Site-directed mutagenesis experiments reported in the literature³⁸ have shown that both His199 and Met276 are important for binding the non-peptide high-affinity CRF-1 receptor antagonist *N*-(3-(2,4-dimethoxyphenyl)-2,5-dimethylpyrazolo[1,5-*a*]pyrimidin-7-yl)-*N*-(2-methoxyethyl)-*N*-propylamine hydrochloride (NBI27914),³⁸ suggesting that TM regions make the binding pocket for nonpeptidic antagonists. In addition, the nitrogen present in the 2-thiazole, 1-pyrazole, and 2-pyridyl fragments should lie close to Thr192 and to Tyr195, underlying the possibility of making both H-bond acceptor interaction and aromatic–aromatic contacts with these residues. Furthermore,

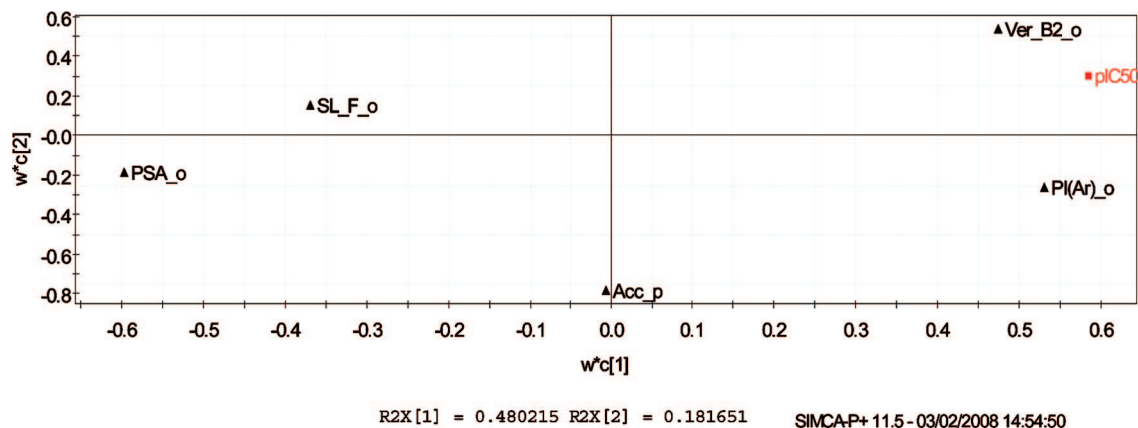


Figure 3. Model_M2 loadings plot. First component accounts mainly for the effects of the ortho substituent on the activity: shape (Ver_B2_o) and lipophilicity (PI(Ar)_o) positive contribution, electronic inductive (SL_F_o) and polarity (PSA_o) negative contribution; the second component for the shape of the ortho substituent (positive contribution) and number of hydrogen bond acceptors (Acc_p) in para position (negative contribution).

Table 2. MRL-like Equation (M2) Coefficients

parameter	M2 coefficient
constant	4.401
PI(Ar)_o	0.440
SL_F_o	-0.514
Ver_B2_o	1.226
PSA_o	-0.024
Acc_p	-0.401

as shown in Figure 6B, the 2-thiazole ring can make hydrophobic contacts with Leu329 in TM6 and is also projected toward Glu352 in TM7, which in turn makes H-bond interactions with Asn333 in TM6.

As far as the pendent phenyl ring is concerned, the observed effects for the ortho substituents discussed above seem in agreement with the docking model in which this portion of the molecule lies in a lipophilic pocket whose shape and size are modeled by Leu322 and Phe198.

For the effects of the substituents present in the para position of our docking model studies, the prediction of the presence of a relatively polar pocket (Asn283, Asn202) is not fully corroborated by the results of the QSAR analysis, claiming instead for the presence of a nonpolar receptor pocket of limited size. However, although hydrophobic residues are also supposed to be present in this region (i.e., Val279), enabling interpretation of the observed discrepancy, the information available to date is considered limited and additional site direct mutagenesis (SDM) experiments are necessary to make a more valid hypothesis on the nature of the receptor binding pocket accommodating the para substituent of the pendent phenyl ring.

Conclusions

In summary, we presented herein the results of the exploration performed on the dihydropyrrole[2,3]pyridine series aimed at identifying novel CRF-1 receptor antagonists. Selective and potent compounds have been discovered, endowed with reduced ClogP with respect to compounds known in the literature. Of particular relevance was the observation that by reduction of the overall lipophilicity of the molecules by modifying the top region of this template and/or the substitution of the pendent phenyl ring and increasing the basicity of the aromatic nitrogen, the *in vitro* affinity of the series was maintained. These encouraging results were explained by QSAR analysis of the substituents of the pendent phenyl ring. Moreover, a representative example of this series was docked in a putative *in silico*

nonpeptidic antagonist binding site set up in house by homology modeling techniques. The latter studies seem to clarify the SAR observed for this series of CRF-1 receptor antagonists, confirming the critical role of appropriate H-bond acceptors in the top region of the molecule correctly positioned within space (2-thiazole, 2-pyridine, or 1-pyrazole). These new hypotheses on the CRF-1 receptor antagonists binding pocket might be useful to expand further the exploration of the top region of these molecules, seeking more hydrophilic, druggable series of CRF-1 receptor antagonists, an area still associated with relevant challenge in modern medicinal chemistry.

Experimental Section

Docking Experiments. Flexible docking experiments in the putative binding site of the CRF1 receptor model were carried out with routines (MCMM) implemented in MacroModel/Batchmin (ref 37). Random sampling was performed for 2K steps followed by energy minimization of the complexes sampled with the AMBER* united atom force field (1K steps). ESP charges (AM1 Hamiltonian, MOPAC) were utilized for the ligands, while charges from the force field were used for the protein.

QSAR Modeling. PLS was performed using the package SIMCA-P 10.5 (Umetrics AB, Umeå, Sweden). The number of significant PCs was determined by 1000 internal cross-validation rounds (i.e., leave anything out each time), and the fraction of explained variation (R^2 or "goodness of fit") and the fraction of predicted variation of Y (Q^2 or "goodness of prediction") were calculated. The PLS model was also validated by random permutation (100 times) of the Y values, and separate models were fitted to these permuted Y values by extracting the same number of PCs as was done in the original model. A plot of the correlation coefficients between the original and permuted Y values against R^2 and Q^2 gives a measure of overfitting. None of the PLS models were overfitted according to this validation method (not shown). All X and Y variables were centered and scaled to unit variance.

Physicochemical descriptors Dy_lip, ClogP-north, ClogP (partition coefficient in octanol/water of the neutral species), and the difference in $\log P$ for the benzene and pyridine pendant ring, 2-thiazole replacement, and $\log P$ of the whole molecule were calculated using the program ClogP v (Daylight Software). Acceptors, Acc_o, and Acc_p are the total number of hydrogen bond acceptors in the ortho and para positions. Sigma(meta), Sigma(para), Sigma(Res-) are electronic substituent parameters, as calculated by ACD/Sigma, and refer to Sigma inductive, Sigma resonance (π -electron delocalization, benzoic acid model), Sigma meta for substituent in the meta position on an aromatic ring (derived from benzoic acids), Sigma para for substituent in the para position on an aromatic ring (derived from benzoic acids), Sigma aniline

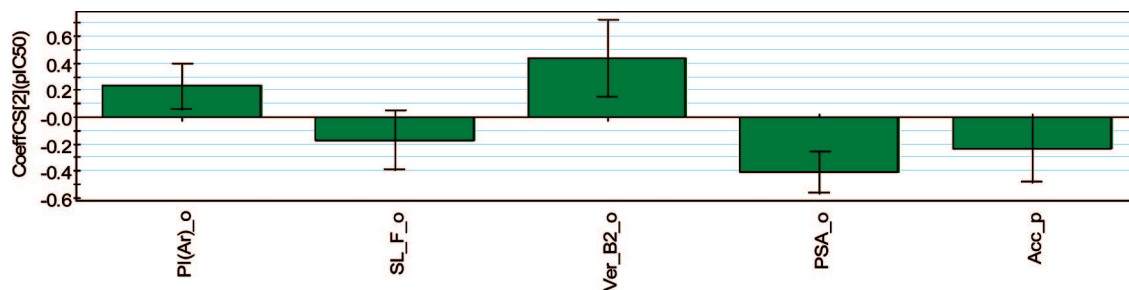


Figure 4. M2 coefficient plot (scaled and centered).

Table 3

parameter	value
<i>n</i>	31
<i>A</i>	2
<i>s</i>	0.35
<i>R</i> ²	0.87
<i>Q</i> ²	0.80
variables included	6 (<i>x</i> = 5, <i>y</i> = 1)

resonance (π -electron delocalization, aniline model), and Sigma plus resonance (π -electron delocalization from *tert*-cumyl chlorides), respectively. MR (cm³), MV (cm³), Pi (Hansch hydrophobic constant π), MW (molecular weight) were also used.

Synthetic Chemistry: General Methods. ¹H NMR spectra were recorded on a Varian Mercury (300 MHz) or a Bruker Avance (400 MHz) spectrometers in CDCl₃, DMSO-*d*₆, or CD₃OD solution unless otherwise stated. Chemical shifts are reported in parts per million (ppm) referencing the CHCl₃ residual line as an internal standard (δ = 7.26 ppm), the DMSO residual line (δ = 2.49 ppm), or CD₃OD residual line (δ = 3.34 ppm) and are assigned as singlets (s), doublets (d), triplets (t), quadruplets (q), or multiplets (m). Full assignment of ¹H and ¹³C for compound 7 (600 MHz) is included. Mass spectral analyses were performed on a VG Platform (Waters, Manchester, U.K.) mass spectrometer operating in positive electrospray ion mode. Analytical thin layer chromatography (TLC) was performed on glass plates (Merck Kieselgel 60 F₂₅₄). Visualization was accomplished by UV light (254 nm) or I₂. Column chromatography was performed on silica gel (Merck Kieselgel 70–230 mesh). All reactions were carried out under anhydrous nitrogen using standard Schlenk techniques. Most chemicals and solvents were analytical grade and used without further purification.

General Synthetic Procedures: Synthesis of Compounds 4–39 (See Scheme 1). Step a. To a solution of substituted 1*H*-pyrazol-3-yl derivatives (1.05 equiv) in dry DMF at 0 °C under N₂ atmosphere, NaH 60% in mineral oil (1.05 equiv) was added, and the reaction mixture was stirred for 10 min at 0 °C and then for 1 h at room temperature. Then, compound 47 (1 equiv) dissolved in dry DMF was added at 0 °C. The resulting solution was heated at 110 °C for 3 h. After aqueous workup and chromatographic purification, compounds 48 were isolated.

Step b. Intermediates 48 were dissolved into CH₂Cl₂ and reacted at –78 °C under N₂ atmosphere, with DIBAL-H 1 M in cyclohexane (3.0 equiv). After aqueous workup the crude mixtures were purified by flash chromatography to give compounds 49.

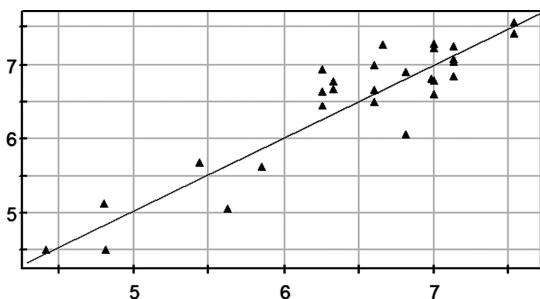


Figure 5. CRF-1 pIC₅₀ predicted (*X*) versus observed (*Y*).

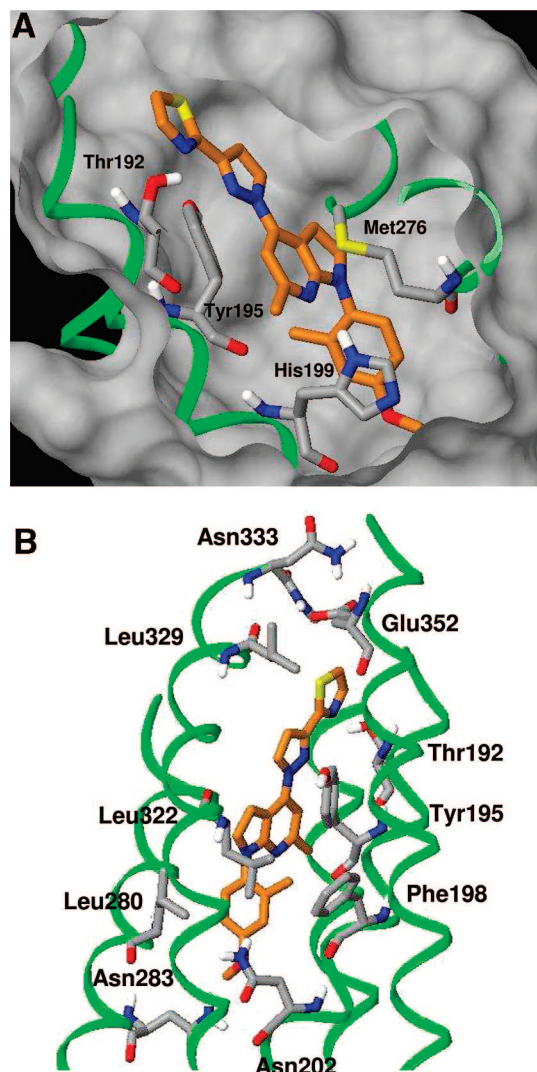


Figure 6. (A) Energetically favorable docking solution obtained for compound 7, showing details of the amino acid residues potentially interacting with the bicycle core and the heterocycle groups present in the upper region of the molecule. (B) Additional amino acid residues potentially interacting with compound 7.

Step c. To a solution of compounds 49 in dry CH₂Cl₂ at room temperature under N₂ atmosphere Dess–Martin's reagent (1.1 equiv) was added, and the reaction mixture was stirred for 1 h at room temperature. The reaction was then quenched with a solution of 0.5 M of Na₂S₂O₃, dissolved in saturated NaHCO₃, and extracted with EtOAc. The organic extracts were collected and washed with brine, dried (Na₂SO₄), filtered, and concentrated in vacuo. The crude products were purified by flash chromatography to afford the aldehyde derivatives 50.

Step d. *n*-BuLi (1.6 M) in cyclohexane (3 equiv) was added to a solution of (methoxymethyl)triphenylphosphonium chloride (3

equiv) in dry THF at 0 °C under N₂ atmosphere, and the reaction mixture was brought to room temperature and stirred for 15 min. Compounds **50** (1 equiv) were dissolved in dry THF and added to the reaction mixture, then stirred for 1.5 h at room temperature. The reaction mixture was partitioned between brine and ethyl acetate. The organic layer was dried (Na₂SO₄), filtered, and concentrated in vacuo. The crude residue was purified by flash chromatography to afford the corresponding enol ether intermediate, which was dissolved in THF followed by addition of 6 N HCl (45 equiv). The reaction mixture was stirred at room temperature for 15 h. Ethyl acetate was added, and the organic layer was washed with brine, dried (Na₂SO₄), filtered, and concentrated in vacuo. The crude residue was used in the next step without further purification.

Steps e and f. To a solution of compounds **51** dissolved in dry MeOH, CeCl₃ (1 equiv) and NaBH₄ (1 equiv) were added, and the reaction mixture was stirred for 5 min at room temperature. The reaction was quenched with H₂O, and the aqueous layer was extracted with AcOEt. The organic extracts were washed with brine, dried (Na₂SO₄), filtered, and concentrated in vacuo to afford compounds **52**, which were dissolved in dry CH₂Cl₂ and treated with 2,6-lutidine (2.2 equiv) and *tert*-butyldimethylsilyl triflate (1.5 equiv) and stirred 15 h at room temperature. The reaction was then quenched with saturated NH₄Cl and extracted with ethyl acetate. The organic extracts were washed with brine, dried (Na₂SO₄), filtered, and concentrated in vacuo. The crude residue was then purified by flash chromatography to give compounds **53**.

Steps g and h. Compounds **53** were dissolved in dry DME and Pd₂(dba)₃ (0.1 equiv), 2-(dicyclohexylphosphino)-2'-methylbiphenyl (0.3 equiv), and K₃PO₄ (3 equiv). The substituted aniline/aminopyridine derivatives (1.2 equiv) were added. Then, the reaction mixture was irradiated two times (20 min each) in a microwave apparatus (150 W, 100 °C, 60 psi). The reaction mixture was poured in H₂O and extracted with ethyl acetate. The organic extracts were dried (Na₂SO₄), filtered, and concentrated in vacuo and purified by flash chromatography to afford the compounds **54**. These intermediates were then dissolved in THF. Et₃N·3HF (3 equiv) was added, and the reaction mixture was stirred for 15 h at room temperature. The desired compounds **55** were isolated after aqueous workup and purification by flash chromatography.

Step i. To a solution of **55** in dry DMF were added at room temperature Et₃N (4 equiv) and MsCl (2 equiv). The solution was stirred at 56 °C for 4 h. CH₂Cl₂ was added, and the mixture was poured into H₂O. The aqueous layer was extracted with CH₂Cl₂ and dried (Na₂SO₄). After filtration and evaporation of the solvent in vacuo the crude product was purified by flash chromatography to give the title compounds. Alternatively, intermediate **55** was then dissolved in dry CH₂Cl₂. Et₃N (4 equiv), PPh₃ (4 equiv), and I₂ (4 equiv) or CBr₄ were added at room temperature. The reaction mixture was stirred at room temperature for 2 h. After workup the crude residue was purified by flash chromatography to give the title compounds.

1-(2,4-Bis-trifluoromethylphenyl)-6-methyl-4-(3-thiazol-2-ylpyrazol-1-yl)-2,3-dihydro-1H-pyrrolo[2,3-*b*]pyridine (4). ¹H NMR (400 MHz, DMSO): δ 8.64 (d, 1H), 8.17 (dd, 1H), 8.13 (d, 1H), 7.94 (d, 1H), 7.84 (d, 1H), 7.80 (d, 1H), 7.09 (m, 2H), 3.97 (t, 2H), 3.56 (t, 2H), 2.24 (s, 3H). MS (*m/z*): 496 [MH]⁺.

6-Methyl-1-[4-nitro-2-(trifluoromethyl)phenyl]-4-[3-(1,3-thiazol-2-yl)-1H-pyrazol-1-yl]-2,3-dihydro-1H-pyrrolo[2,3-*b*]pyridine (5). ¹H NMR (400 MHz, CDCl₃): δ 8.63 (d, 1H), 8.41 (dd, 1H), 8.03 (d, 1H), 7.90 (d, 1H), 7.76 (d, 1H), 7.37 (d, 1H), 7.10 (d, 1H), 6.85 (s, 1H), 4.08 (t, 2H), 3.65 (t, 2H), 2.40 (s, 3H). MS (*m/z*): 473 [MH]⁺.

4-[6-Methyl-4-(3-thiazol-2-ylpyrazol-1-yl)-2,3-dihydro-1H-pyrrolo[2,3-*b*]pyridin-1-yl]-3-trifluoromethylbenzotrile (6). ¹H NMR (300 MHz, CDCl₃): δ 8.00 (m, 2H), 7.9–7.8 (d + d, 2H), 7.65 (d, 1H), 7.35 (d, 1H), 7.10 (d, 1H), 6.80 (s, 1H), 4.00 (t, 2H), 3.60 (t, 2H), 3.56 (t, 2H), 2.40 (s, 3H). MS (*m/z*): 453 [MH]⁺.

1-(4-Methoxy-2-methylphenyl)-6-methyl-4-(3-thiazol-2-ylpyrazol-1-yl)-2,3-dihydro-1H-pyrrolo[2,3-*b*]pyridine (7). ¹H NMR (600 MHz, Varian Inova, DMSO-*d*₆) δ 8.58 (d, *J* = 2.47 Hz, 1H), 7.94 (d, *J* = 3.30 Hz, 1H), 7.80 (d, *J* = 3.30 Hz, 1H), 7.19 (d, *J* = 8.51

Hz, 1H), 7.07 (d, *J* = 2.75 Hz, 1H), 6.88 (d, *J* = 3.02, 1H), 6.87 (s, 1H), 6.81 (dd, *J* = 3.02, 8.51 Hz, 1H), 3.90 (t, 2H), 3.76 (s, 3H), 3.50 (t, 2H), 2.23 (s, 3H), 2.17 (s, 3H). ¹³C NMR (150.81 MHz, Varian Inova, DMSO-*d*₆) δ ppm 163.63, 160.25, 157.47, 156.33, 147.83, 143.49, 141.18, 137.30, 133.55, 131.31, 127.42, 120.44, 115.73, 111.94, 108.44, 105.58, 102.07, 55.17, 51.56, 26.47, 23.93, 18.33. MS (*m/z*): 404 [MH]⁺. Anal. Calcd for C₂₂H₂₁N₅O₅: C, 65.49%; H, 5.25%; N, 17.36%. Found: C, 65.60%; H, 5.28%; N, 17.33%.

3-Methyl-4-[6-methyl-4-(3-thiazol-2-ylpyrazol-1-yl)-2,3-dihydro-1H-pyrrolo[2,3-*b*]pyridin-1-yl]benzotrile (8). ¹H NMR (400 MHz, DMSO): δ 8.02 (d, 1H), 7.90 (d, 1H), 7.59 (d, 1H), 7.53 (dd, 1H), 7.41 (d, 1H), 7.38 (d, 1H), 6.76 (s, 1H), 4.04 (t, 2H), 3.62 (t, 2H), 2.41 (s, 3H), 2.33 (s, 3H). MS (*m/z*): 399 [MH]⁺.

6-Methyl-1-[2-methyl-4-(1H-pyrazol-1-yl)phenyl]-4-[3-(1,3-thiazol-2-yl)-1H-pyrazol-1-yl]-2,3-dihydro-1H-pyrrolo[2,3-*b*]pyridine (9). ¹H NMR (300 MHz, CDCl₃): δ 7.99 (d, 1H), 7.89 (d, 1H), 7.87 (d, 1H), 7.70 (d, 1H), 7.63 (d, 1H), 7.52 (dd, 1H), 7.35 (d, 1H), 7.34 (d, 1H), 7.06 (d, 1H), 6.66 (s, 1H), 6.44 (t, 1H), 3.98 (t, 2H), 3.57 (t, 2H), 2.36 (s, 3H), 2.33 (s, 3H). MS (*m/z*): 440 [MH]⁺.

1-(4-Fluoro-2-methylphenyl)-6-methyl-4-[3-(1,3-thiazol-2-yl)-1H-pyrazol-1-yl]-2,3-dihydro-1H-pyrrolo[2,3-*b*]pyridine (10). ¹H NMR (300 MHz, CDCl₃): δ 7.98 (d, 1H), 7.88 (d, 1H), 7.36 (d, 1H), 7.25 (m, 1H), 7.06 (d, 1H), 7.02/6.9 (m, 2H), 6.57 (s, 1H), 3.93 (t, 2H), 3.56 (t, 2H), 2.36 (s, 3H), 2.27 (s, 3H). MS (*m/z*): 392 [MH]⁺.

3-Methyl-4-(6-methyl-4-[3-(1,3-thiazol-2-yl)-1H-pyrazol-1-yl]-2,3-dihydro-1H-pyrrolo[2,3-*b*]pyridin-1-yl)phenol (11). ¹H NMR (300 MHz, CDCl₃): δ 11.15 (s, 1H), 7.96 (d, 1H), 7.90 (d, 1H), 7.36 (d, 1H), 7.06 (d, 1H), 6.89 (d, 1H), 6.58 (s, 1H), 6.41 (d, 1H), 6.39 (d, 1H), 3.87 (t, 2H), 3.65 (t, 2H), 2.46 (s, 3H), 2.12 (s, 3H). MS (*m/z*): 390.4 [MH]⁺.

1-[4-(3,5-Dimethyl-4-isoxazolyl)-2-methylphenyl]-6-methyl-4-[3-(1,3-thiazol-2-yl)-1H-pyrazol-1-yl]-2,3-dihydro-1H-pyrrolo[2,3-*b*]pyridine (12). ¹H NMR (300 MHz, CDCl₃): δ 8.02 (d, 1H), 7.89 (d, 1H), 7.38 (m, 2H), 7.20–7.00 (m, 3H), 6.63 (s, 1H), 4.00 (t, 2H), 3.59 (t, 2H), 2.43 (s, 3H), 2.41 (s, 3H), 2.17 (s, 3H), 2.16 (s, 3H). MS (*m/z*): 469.5 [MH]⁺.

6-Methyl-1-(2-methyl-4-trifluoromethoxyphenyl)-4-(3-thiazol-2-ylpyrazol-1-yl)-2,3-dihydro-1H-pyrrolo[2,3-*b*]pyridine (13). ¹H NMR (400 MHz, CDCl₃): δ 8.01 (d, 1H), 7.89 (d, 1H), 7.5 (d, 1H), 7.45 (dd, 1H), 7.20 (d, 1H), 7.1 (dd, 2H), 6.65 (s, 1H), 3.9 (t, 2H), 3.56 (t, 2H), 2.32 (s, 3H), 2.2 (s, 3H). MS (*m/z*): 458.5 [MH]⁺.

3-Ethyl-4-(6-methyl-4-[3-(1,3-thiazol-2-yl)-1H-pyrazol-1-yl]-2,3-dihydro-1H-pyrrolo[2,3-*b*]pyridin-1-yl)benzotrile (14). ¹H NMR (300 MHz, DMSO): δ 9.17 (s, 1H), 8.32 (d, 1H), 7.98 (d, 1H), 7.92 (s, 1H), 7.75 (s, 1H), 7.60 (s, 1H), 7.54 (d, 1H), 7.03 (s, 2H), 7.96 (s, 1H), 4.01 (t, 2H), 3.23 (t, 2H), 2.64 (q, 2H), 2.41 (s, 3H), 1.40 (t, 3H). MS (*m/z*): 414 [MH]⁺.

1-[2,4-Bis(methoxy)phenyl]-6-methyl-4-[3-(1,3-thiazol-2-yl)-1H-pyrazol-1-yl]-2,3-dihydro-1H-pyrrolo[2,3-*b*]pyridine (15). ¹H NMR (400 MHz, CDCl₃): δ 7.97 (d, 1H), 7.86 (d, 1H), 7.34 (d, 1H), 7.04 (d, 1H), 6.64 (s, 1H), 6.54 (d, 1H), 6.51 (d, 1H), 3.82 (s, 3H), 3.79 (s, 3H), 3.53–3.46 (m, 4H), 2.36 (s, 3H). MS (*m/z*): 421 [MH]⁺.

4-(6-Methyl-4-[3-(1,3-thiazol-2-yl)-1H-pyrazol-1-yl]-2,3-dihydro-1H-pyrrolo[2,3-*b*]pyridin-1-yl)-3-[(trifluoromethyl)oxy]benzotrile (16). ¹H NMR (400 MHz, CDCl₃): δ 8.66 (d, 1H), 8.03 (s, 1H), 7.96 (d, 1H), 7.94 (d, 1H), 7.88 (dd, 1H), 7.81 (d, 1H), 7.21 (s, 1H), 7.10 (d, 1H), 4.16 (t, 2H), 3.56 (t, 2H), 2.35 (s, 3H). MS (*m/z*): 469 [MH]⁺.

1-(2-Chloro-4-methoxyphenyl)-6-methyl-4-[3-(1,3-thiazol-2-yl)-1H-pyrazol-1-yl]-2,3-dihydro-1H-pyrrolo[2,3-*b*]pyridine (17). ¹H NMR (300 MHz, CDCl₃): δ 7.97 (bs, 1H), 7.86 (bs, 1H), 7.36–7.32 (m, 2H), 7.01 (d, 2H), 6.85 (m, 1H), 6.66 (s, 1H), 3.96 (t, 2H), 3.79 (s, 3H), 3.54 (t, 2H), 2.35 (s, 3H). MS (*m/z*): 424 [MH]⁺.

3-Chloro-4-(6-methyl-4-[3-(1,3-thiazol-2-yl)-1H-pyrazol-1-yl]-2,3-dihydro-1H-pyrrolo[2,3-*b*]pyridin-1-yl)benzotrile (18). ¹H NMR (300 MHz, CDCl₃): δ 8.02 (d, 1H), 7.90 (d, 1H), 7.74 (d, 1H), 7.73 (d, 1H), 7.56 (dd, 1H), 7.37 (d, 1H), 7.09 (d, 1H), 6.83 (s, 1H), 4.16 (t, 2H), 3.62 (t, 2H), 2.43 (s, 3H). MS (*m/z*): 419 [MH]⁺.

1-[2-Chloro-4-(methylsulfonyl)phenyl]-6-methyl-4-[3-(1,3-thiazol-2-yl)-1H-pyrazol-1-yl]-2,3-dihydro-1H-pyrrolo[2,3-b]pyridine (19). ¹H NMR (300 MHz, CDCl₃): δ 8.06 (m, 2H), 7.93 (d, 1H), 7.86 (m, 2H), 7.40 (d, 1H), 7.12 (d, 1H), 6.88 (s, 1H), 4.21 (t, 2H), 3.66 (t, 2H), 3.12 (s, 3H), 2.47 (s, 3H). MS (*m/z*): 472.9 [MH]⁺.

4-(6-Methyl-4-[3-(1,3-thiazol-2-yl)-1H-pyrazol-1-yl]-2,3-dihydro-1H-pyrrolo[2,3-b]pyridin-1-yl)-3-(2-thienyl)benzotrile (20). ¹H NMR (300 MHz, CDCl₃): δ 7.93 (d, 1H), 7.85 (d, 1H), 7.78 (d, 1H), 7.67 (d, 1H), 7.55 (dd, 1H), 7.31 (d, 1H), 7.27 (d, 1H), 7.22 (d, 1H), 7.03 (d, 1H), 6.99 (dd, 1H), 6.71 (s, 1H), 3.67 (t, 2H), 3.40 (t, 2H), 2.38 (s, 3H). MS (*m/z*): 467.5 [MH]⁺.

4-(6-Methyl-4-[3-(1,3-thiazol-2-yl)-1H-pyrazol-1-yl]-2,3-dihydro-1H-pyrrolo[2,3-b]pyridin-1-yl)-1,3-benzenedicarbonitrile (21). ¹H NMR (400 MHz, CDCl₃): δ 8.03 (m, 2H), 7.95 (m, 2H), 7.88 (dd, 1H), 7.39 (d, 1H), 7.09 (d, 1H), 6.95 (s, 1H), 4.40 (t, 2H), 3.42 (t, 2H), 2.51 (s, 3H). MS (*m/z*): 410.4 [MH]⁺.

1-(4-Fluoro-2-nitrophenyl)-6-methyl-4-[3-(1,3-thiazol-2-yl)-1H-pyrazol-1-yl]-2,3-dihydro-1H-pyrrolo[2,3-b]pyridine (22). ¹H NMR (300 MHz, CD₃OD): δ 9.35 (d, 1H), 8.77 (d, 1H), 7.98 (d, 1H), 7.80–7.71 (m, 2H), 7.49 (m, 2H), 7.11 (s, 1H), 5.44 (t, 2H), 3.12 (t, 2H), 2.25 (s, 3H). MS (*m/z*): 423.4 [MH]⁺.

1-(4-Chloro-2-nitrophenyl)-6-methyl-4-[3-(1,3-thiazol-2-yl)-1H-pyrazol-1-yl]-2,3-dihydro-1H-pyrrolo[2,3-b]pyridine (23). ¹H NMR (300 MHz, CD₃OD): δ 9.27 (d, 1H), 8.59 (d, 1H), 8.27 (d, 1H), 8.21 (d, 1H), 8.14 (d, 1H), 7.72 (d, 1H), 7.68 (dd, 1H), 7.47 (s, 1H), 5.47 (t, 2H), 3.37 (t, 2H), 2.55 (s, 3H). MS (*m/z*): 439.9 [MH]⁺.

4-(6-Methyl-4-[3-(1,3-thiazol-2-yl)-1H-pyrazol-1-yl]-2,3-dihydro-1H-pyrrolo[2,3-b]pyridin-1-yl)-3-nitrobenzotrile (24). ¹H NMR (400 MHz, DMSO): δ 10.07 (s, 1H), 9.52 (d, 1H), 8.55 (d, 1H), 8.36 (s, 2H), 8.07 (dd, 1H), 8.02–7.99 (m, 2H), 7.68 (s, 1H), 5.31 (t, 2H), 3.37 (t, 2H), 2.57 (s, 3H). MS (*m/z*): 430.4 [MH]⁺.

6-Methyl-1-[4-(methoxy)-2-nitrophenyl]-4-[3-(1,3-thiazol-2-yl)-1H-pyrazol-1-yl]-2,3-dihydro-1H-pyrrolo[2,3-b]pyridine (25). ¹H NMR (300 MHz, CD₃OD): δ 9.22 (d, 1H), 8.29 (d, 1H), 8.12 (d, 1H), 8.00 (d, 1H), 7.61 (m, 2H), 7.20–7.13 (m, 2H), 5.37 (t, 2H), 3.79 (s, 3H), 3.42 (t, 2H), 2.56 (s, 3H). MS (*m/z*): 435.4 [MH]⁺.

1-[2,4-Bis(methylsulfonyl)phenyl]-6-methyl-4-[3-(1,3-thiazol-2-yl)-1H-pyrazol-1-yl]-2,3-dihydro-1H-pyrrolo[2,3-b]pyridine (26). ¹H NMR (300 MHz, CDCl₃): δ 8.75 (d, 1H), 8.25 (dd, 1H), 8.05 (d, 1H), 7.90 (d, 1H), 7.65 (d, 1H), 7.40 (d, 1H), 7.10 (d, 1H), 6.85 (s, 1H), 4.10 (t, 2H), 3.65 (t, 2H), 3.25 (s, 3H), 3.10 (s, 3H), 2.35 (s, 3H). MS (*m/z*): 516.6 [MH]⁺.

1-(2-Difluoromethyl-4-methoxyphenyl)-6-methyl-4-[3-(1,3-thiazol-2-yl)-1H-pyrazol-1-yl]-2,3-dihydro-1H-pyrrolo[2,3-b]pyridine (27). ¹H NMR (400 MHz, CDCl₃): δ 8.00 (d, 1H), 7.89 (d, 1H), 7.36 (d, 1H), 7.24 (m, 2H), 7.08 (m, 2H), 6.88 (t, 1H), *J*_{H-F} = 55.8 Hz, 6.71 (s, 1H), 3.95 (t, 2H), 3.87 (s, 3H), 3.56 (t, 2H), 2.36 (s, 3H). MS (*m/z*): 440 [MH]⁺.

6-Methyl-1-[4-(methoxy)phenyl]-4-[3-(1,3-thiazol-2-yl)-1H-pyrazol-1-yl]-2,3-dihydro-1H-pyrrolo[2,3-b]pyridine (28). ¹H NMR (400 MHz, DMSO): δ 8.57 (d, 1H), 7.90 (d, 1H), 7.77 (d, 2H), 7.75 (d, 1H), 7.03 (d, 1H), 6.98 (s, 1H), 6.91 (d, 2H), 4.03 (t, 2H), 3.70 (s, 3H), 3.46 (t, 2H), 2.36 (s, 3H). MS (*m/z*): 390.4 [MH]⁺.

3-Fluoro-4-(6-methyl-4-[3-(1,3-thiazol-2-yl)-1H-pyrazol-1-yl]-2,3-dihydro-1H-pyrrolo[2,3-b]pyridin-1-yl)benzotrile (29). ¹H NMR (300 MHz, CDCl₃): δ 8.19 (dd, 1H), 8.00 (d, 1H), 7.86 (d, 1H), 7.42 (d, 1H), 7.35 (m, 2H), 7.12 (d, 1H), 6.85 (s, 1H), 4.18 (t, 2H), 3.62 (t, 2H), 2.35 (s, 3H). MS (*m/z*): 403.4 [MH]⁺.

6-Methyl-1-[2-methyl-6-(methoxy)-3-pyridinyl]-4-[3-(1,3-thiazol-2-yl)-1H-pyrazol-1-yl]-2,3-dihydro-1H-pyrrolo[2,3-b]pyridine (30). ¹H NMR (300 MHz, CDCl₃): δ 7.98 (d, 1H), 7.88 (d, 1H), 6.98 (d, 1H), 6.83 (d, 1H), 7.03 (d, 1H), 6.62 (d, 1H), 6.60 (s, 1H), 3.92 (s, 3H), 3.90 (d, 2H), 3.56 (d, 2H), 2.39 (s, 3H), 2.35 (s, 3H). MS (*m/z*): 405 [MH]⁺.

1-[2,6-Bis(methoxy)-3-pyridinyl]-6-methyl-4-[3-(1,3-thiazol-2-yl)-1H-pyrazol-1-yl]-2,3-dihydro-1H-pyrrolo[2,3-b]pyridine (31). ¹H NMR (300 MHz, CDCl₃): δ 7.98 (d, 1H), 7.87 (d, 1H), 7.72 (d, 1H), 7.34 (d, 1H), 7.06 (d, 1H), 6.67 (s, 1H), 6.36 (d, 1H), 3.96 (t, 2H), 3.96 (s, 3H), 3.94 (s, 3H), 3.51 (t, 2H), 2.37 (s, 3H). MS (*m/z*): 421 [MH]⁺.

6-Methyl-1-[6-(methoxy)-2-(trifluoromethyl)-3-pyridinyl]-4-[3-(1,3-thiazol-2-yl)-1H-pyrazol-1-yl]-2,3-dihydro-1H-pyrrolo[2,3-b]pyridine (32). ¹H NMR (400 MHz, CDCl₃): δ 7.9 (d, 1H), 7.8 (d, 1H), 7.6 (d, 1H), 7.3 (d, 1H), 7.0 (d, 1H), 6.9 (d, 1H), 6.7 (s, 1H), 3.9 (s, 3H), 3.8 (t, 2H), 3.5 (t, 2H), 2.33 (s, 3H). MS (*m/z*): 459 [MH]⁺.

N,N,4-Trimethyl-5-(6-methyl-4-[3-(1,3-thiazol-2-yl)-1H-pyrazol-1-yl]-2,3-dihydro-1H-pyrrolo[2,3-b]pyridin-1-yl)-2-pyridinamine (33). ¹H NMR (400 MHz, CDCl₃): δ 8.57 (d, 1H), 7.95 (s, 1H), 7.92 (d, 1H), 7.78 (d, 1H), 7.04 (d, 1H), 6.86 (s, 1H), 6.55 (s, 1H), 3.88 (t, 2H), 3.49 (t, 2H), 3.16 (s, 3H), 3.14 (s, 3H), 3.01 (s, 6H). MS (*m/z*): 418 [MH]⁺.

3-Chloro-4-(6-methyl-4-[3-(2-pyridinyl)-1H-pyrazol-1-yl]-2,3-dihydro-1H-pyrrolo[2,3-b]pyridin-1-yl)benzotrile (34). ¹H NMR (300 MHz, CDCl₃): δ 8.67 (d, 1H), 8.11 (d, 1H), 8.03 (d, 1H), 7.75 (m, 2H), 7.75 (m, 1H), 7.55 (dd, 1H), 7.26 (m, 1H), 7.2 (d, 1H), 6.88 (s, 1H), 4.16 (t, 2H), 3.65 (t, 2H), 2.43 (s, 3H). MS (*m/z*): 413 [MH]⁺.

3-Methyl-4-(6-methyl-4-[3-(2-pyridinyl)-1H-pyrazol-1-yl]-2,3-dihydro-1H-pyrrolo[2,3-b]pyridin-1-yl)benzotrile (35). ¹H NMR (300 MHz, CDCl₃): δ 8.65 (dd, 1H), 8.10 (d, 1H), 8.00 (d, 1H), 7.75 (dt, 1H), 7.55–7.48 (m, 2H), 7.39 (d, 1H), 7.26 (m, 1H), 7.15 (d, 1H), 6.78 (s, 1H), 4.00 (t, 2H), 3.60 (t, 2H), 2.37 (s, 3H), 2.31 (s, 3H). MS (*m/z*): 393 [MH]⁺.

4-(6-Methyl-4-[3-(2-pyridinyl)-1H-pyrazol-1-yl]-2,3-dihydro-1H-pyrrolo[2,3-b]pyridin-1-yl)-3-(trifluoromethyl)benzotrile (36). ¹H NMR (300 MHz, CDCl₃): δ 8.66 (dd, 1H), 8.10 (d, 1H), 8.02 (d, 1H), 8.00 (d, 1H), 7.84 (dd, 1H), 7.76 (t, 1H), 7.69 (d, 1H), 7.27 (t, 1H), 7.18 (d, 1H), 6.87 (s, 1H), 4.02 (t, 2H), 3.64 (t, 2H), 2.38 (s, 3H). MS (*m/z*): 447 [MH]⁺.

4-[4-(1'H-1,3'-Bipyrazol-1'-yl)-6-methyl-2,3-dihydro-1H-pyrrolo[2,3-b]pyridin-1-yl]-3-methylbenzotrile (37). ¹H NMR (400 MHz, CDCl₃): δ 8.2 (d, 1H), 8.0 (d, 1H), 7.7 (d, 1H), 7.6 (d, 1H), 7.5 (dd, 1H), 7.4 (dd, 1H), 6.8 (d, 1H), 6.7 (d, 1H), 6.4 (t, 1H), 4.0 (t, 2H), 4.0 (t, 2H), 3.6 (t, 2H), 2.41, 2.35 (s + s, 6H). MS (*m/z*): 382 [MH]⁺.

4-[4-(1'H-1,3'-Bipyrazol-1'-yl)-6-methyl-2,3-dihydro-1H-pyrrolo[2,3-b]pyridin-1-yl]-3-chlorobenzotrile (38). ¹H NMR (400 MHz, CDCl₃): δ 8.2 (d, 1H), 8.0 (d, 1H), 7.8 (m, 3H), 7.6 (d, 1H), 6.8 (m, 2H), 6.4 (d, 1H), 4.2 (t, 2H), 3.6 (t, 2H), 2.40 (s, 3H). MS (*m/z*): 402 [MH]⁺.

4-[4-(1'H-1,3'-Bipyrazol-1'-yl)-6-methyl-2,3-dihydro-1H-pyrrolo[2,3-b]pyridin-1-yl]-3-(trifluoromethyl)benzotrile (39). ¹H NMR (300 MHz, CDCl₃): δ 8.2 (d, 1H), 8.0 (dd, 2H), 7.8 (dd, 1H), 7.7 (d, 1H), 7.6 (dd, 1H), 6.8 (m, 2H), 6.4 (d, 1H), 4.0 (t, 2H), 3.6 (t, 2H), 2.41 (s, 3H). MS (*m/z*): 436 [MH]⁺.

6-Methyl-N-[2-methyl-4-(methoxy)phenyl]-3-[(E)-2-(methoxy)ethenyl]-4-[3-(1,3-thiazol-2-yl)-1H-pyrazol-1-yl]-2-pyridinamine (56). To a solution of (methoxymethyl)triphenylphosphonium chloride (4.24 g, 12.3 mmol) in dry THF (20 mL) at 0 °C under N₂ was added *n*-BuLi (1.6 M) in cyclohexane (7.73 mL, 12.37 mmol), and the reaction mixture was brought to room temperature and then stirred for 15 min. A solution of intermediate **50** (1.25 g, 4.1 mmol) in dry THF (15 mL) was then added, and the mixture was stirred at room temperature for 1.5 h. The reaction was then quenched with water, and the layer was extracted with EtOAc, washed with brine, dried (Na₂SO₄), filtered, and concentrated in vacuo. The crude product was purified by flash chromatography (silica gel, cyclohexane/ethyl acetate 4:1) to give 961 mg of the enol ether intermediate as a white solid (*E/Z* = 3:2 mixture, used as such in the next step). To a solution of this intermediate (180 mg, 0.542 mmol) in dry DME (2 mL) were added Pd₂(dba)₃ (50 mg, 0.054 mmol), K₃PO₄ (270 mg, 1.35 mmol), and 2-methyl-4-(methoxy)aniline (145 μL, 1.08 mmol), and the resulting mixture was submitted to microwave irradiation at 100 °C for 10 min. The reaction mixture was then poured into water and extracted with ethyl acetate. The organic extracts were dried (Na₂SO₄), filtrated, and concentrated in vacuo. The crude material was then purified by flash chromatography (cyclohexane/ethyl acetate from 8:2 to 1:1) to give the target compound (90 mg, 40%). ¹H NMR (300 MHz, CDCl₃): δ 7.79–7.85 (m, 2H), 7.27 (d, 2H), 7.00 (m, 1H),

6.79 (d, 2H), 6.60 (m, 3H), 5.45 (d, 1H), 3.90 (s, 3H), 3.61 (s, 3H), 2.42 (s, 3H), 2.21 (s, 3H). MS (*m/z*): 434.2 [MH]⁺.

6-Methyl-1-[2-methyl-4-(methoxy)phenyl]-4-[3-(1,3-thiazol-2-yl)-1H-pyrazol-1-yl]-1H-pyrrolo[2,3-*b*]pyridine (40). To a solution of intermediate **56** (90 mg, 0.201 mmol) in THF (4 mL), at 0 °C, was added HCl (6 N, 4 mL), and the solution was warmed to room temperature and stirred for 15 h. The reaction was then quenched by the addition of saturated NaHCO₃ and then extracted with ethyl acetate. The organic extracts were collected, dried (Na₂SO₄), filtered, and concentrated in vacuo. The crude material was purified by flash chromatography (cyclohexane/ethyl acetate 7/3) to give the target compound (55 mg, 80%). ¹H NMR (300 MHz, CDCl₃): δ 8.21 (d, 1H), 7.96 (d, 1H), 7.40 (d, 1H), 7.21–7.36 (m, 2H), 7.08–7.20 (dd, 2H), 6.82–6.94 (m, 2H), 6.60 (m, 1H), 3.87 (s, 3H), 3.21 (s, 3H), 2.04 (s, 3H). MS (*m/z*): 402.2 [MH]⁺.

6-Methyl-4-[3-(1,3-thiazol-2-yl)-1H-pyrazol-1-yl]-1H-pyrazolo[3,4-*b*]pyridine (57). To a solution of intermediate **50** (40 mg, 0.132 mmol) in EtOH (2 mL) at room temperature was added hydrazine monohydrate (8 μL, 0.145 mmol, 1.1 equiv), and the mixture was heated in a Sure/Seal vial under microwave irradiation at 100 °C for 10 min. The reaction was quenched with water and extracted with dichloromethane. The organic extracts were dried (Na₂SO₄), filtered, and concentrated in vacuo. The residue was then purified by flash chromatography (cyclohexane/ethyl acetate from 8:2 to 1:1) to give the title compound (20 mg, 54%). ¹H NMR (400 MHz, DMSO-*d*₆): δ 13.61 (br s, 1H), 8.99 (s, 1H), 8.47 (s, 1H), 7.98 (d, 1H), 7.83 (d, 1H), 7.60 (s, 1H), 7.18 (s, 1H), 2.61 (s, 3H). MS (*m/z*): 283.2 [MH]⁺.

3-Methyl-4-(6-methyl-4-[3-(1,3-thiazol-2-yl)-1H-pyrazol-1-yl]-1H-pyrazolo[3,4-*b*]pyridin-1-yl)benzotrile (41). To a solution of intermediate **57** (40 mg, 0.10 mmol) in dioxane (3 mL) were added CuI (10 mg, 0.05 mmol), 1,2-cyclohexanediamine (32 μL, 0.06 mmol), Cs₂CO₃ (80 mg, 0.250 mmol), and 4-bromo-3-methylbenzotrile (40 mg, 0.20 mmol). The resulting reaction mixture was then heated in a Sure/Seal vial at 140 °C for 2 h. The solvent was then evaporated in vacuo and the crude material purified via flash chromatography (cyclohexane/ethyl acetate from 8:2 to 1:1) to give the target compound (2.5 mg, 8%). ¹H NMR (400 MHz, CDCl₃): δ 8.80 (s, 1H), 8.20 (d, 1H), 7.84 (d, 1H), 7.63 (s, 1H), 7.49 (s, 1H), 7.28 (d, 1H), 7.15–7.20 (m, 3H), 2.61 (s, 3H), 2.22 (s, 3H). MS (*m/z*): 398.2 [MH]⁺.

2,4-Dichloro-6-methyl-3-nitropyridine (59). A suspension of the nitropyridone (1 g, 5.88 mmol) in distilled POCl₃ (5.48 mL, 58.8 mmol) was heated, and the solution turned dark-brown. The reaction mixture was refluxed for 3 h, cooled to room temperature, and poured slowly into cold water. Concentrated aqueous NH₄OH was slowly added until pH 8 was attained, and ethyl acetate was added. The organic layer was separated, and the aqueous phase extracted with AcOEt. The combined organic extracts were dried (Na₂SO₄), filtered, and concentrated in vacuo. The black residue was purified by flash chromatography (cyclohexane/ethyl acetate 7:3) to give the desired compound (0.78 g, 64%). ¹H NMR (300 MHz, CDCl₃): δ 7.34 (s, 1H), 2.50 (s, 3H). MS (*m/z*): 207.2 [M]⁺.

2-Chloro-6-methyl-3-nitro-4-[3-(1,3-thiazol-2-yl)-1H-pyrazol-1-yl]pyridine (60). To a suspension of NaH (60% in mineral oil, 41 mg, 1.75 mmol) in dry DMF (2 mL), at room temperature, 2-(1H-pyrazol-3-yl)-1,3-thiazole (170 mg, 1.12 mmol) was added, and the reaction mixture was stirred for 20 min. Compound **59** (212 mg, 1.02 mmol) was added, and the reaction mixture was stirred at room temperature for 90 min. Then it was poured into saturated aqueous NH₄Cl and ethyl acetate. The organic layer was separated, washed with brine, dried (Na₂SO₄), filtered, and concentrated in vacuo. The crude product was purified by flash chromatography (ethyl acetate/cyclohexane 1:1) to give the desired compound as a yellow solid (200 mg, 61%). ¹H NMR (400 MHz, CDCl₃): δ 7.90 (d, 1H), 7.89 (d, 1H), 7.48 (s, 1H), 7.40 (d, 1H), 7.14 (d, 1H), 2.68 (s, 3H). MS (*m/z*): 322.2 [M]⁺.

***N*-[2,4-Bis(trifluoromethyl)phenyl]-6-methyl-3-nitro-4-[3-(1,3-thiazol-2-yl)-1H-pyrazol-1-yl]-2-pyridinamine (61).** Pd₂(dba)₃ (28 mg, 0.031 mmol), dicyclohexyl(2'-methyl-2-biphenyl)phosphane (34 mg, 0.092 mmol), K₃PO₄ (198 mg, 0.92 mmol), 2,4-bis(trif-

luoromethyl)aniline (97 μL, 0.62 mmol), and intermediate **60** (100 mg, 0.31 mmol) were dissolved in dry DME (1 mL). The vial was sealed and irradiated in a microwave apparatus for 20 min (150 W, 100 °C, 60 psi). The reaction mixture was cooled and quenched with saturated aqueous NH₄Cl and extracted with ethyl acetate. The combined organic extracts were dried (Na₂SO₄), filtered, and concentrated in vacuo. The crude residue was purified by column chromatography (cyclohexane/ethyl acetate 3:7) to give the title compound as a yellow oil (17 mg, 11%). ¹H NMR (300 MHz, CDCl₃): δ 9.15 (s, 1H), 8.24 (d, 1H), 7.83 (m, 2H), 7.80 (s, 1H), 7.46 (m, 2H), 7.09 (s, 1H), 6.98 (s, 1H), 2.61 (s, 3H). MS (*m/z*): 515.2 [M]⁺.

***N*²-[2,4-Bis(trifluoromethyl)phenyl]-6-methyl-4-[3-(1,3-thiazol-2-yl)-1H-pyrazol-1-yl]-2,3-pyridinediamine (62).** To a solution of intermediate **61** (17 mg, 0.033 mol) in CH₃CN (0.5 mL) was added water (0.5 mL) at room temperature. The starting material precipitated, and an additional portion of solvent was added (0.5 mL). Then Na₂S₂O₄ (40 mg, 0.231 mmol) was added. The reaction mixture stirred at room temperature for 90 min and then poured into brine and dichloromethane. After separation of the organic layer, the aqueous phase was extracted with dichloromethane. The organic extracts were combined, dried (Na₂SO₄), filtered, and concentrated in vacuo. The crude residue was purified by flash chromatography (cyclohexane/ethyl acetate 3:2) to give the title compound as a yellow solid (4 mg 25%). ¹H NMR (400 MHz, CDCl₃): δ 8.10 (d, 1H), 7.98 (d, 1H), 7.90 (d, 1H), 7.85 (s, 1H), 7.69 (d, 1H), 7.36 (d, 1H), 7.11 (d, 1H), 6.90 (s, 1H), 2.65 (s, 3H). MS (*m/z*): 485.2 [MH]⁺.

3-[2,4-Bis(trifluoromethyl)phenyl]-5-methyl-7-[3-(1,3-thiazol-2-yl)-1H-pyrazol-1-yl]-1,3-dihydro-2H-imidazo[4,5-*b*]pyridin-2-one (42). To a solution of triphosgene (1 mg, 0.008 mmol) and intermediate **62** (4 mg, 0.008 mmol) in anhydrous THF (0.2 mL), at room temperature, triethylamine (7 μL, 0.048 mmol) was added, and the reaction mixture was stirred at room temperature for 3 h. Dichloromethane was added followed by saturated aqueous NaHCO₃. The organic layer was separated, washed with brine, dried (Na₂SO₄), filtered, and concentrated in vacuo. The crude product was purified on a Bond Elut Si cartridge (eluent, gradient from 100:0 to 1:1 cyclohexane/ethyl acetate) to give the target compound as a yellow solid (4 mg, 50%). ¹H NMR (300 MHz, CDCl₃): δ 9.15 (s, 1H), 8.12 (d, 1H), 8.06 (s, 1H), 7.97 (d, 1H), 7.68 (d, 1H), 7.41 (d, 1H), 7.13 (d, 1H), 6.93 (s, 1H), 2.62 (s, 3H). MS (*m/z*): 511.2 [MH]⁺.

3-[2,4-Bis(trifluoromethyl)phenyl]-2,5-dimethyl-7-[3-(1,3-thiazol-2-yl)-1H-pyrazol-1-yl]-3H-imidazo[4,5-*b*]pyridine (43). Intermediate **62** (35 mg, 0.072 mmol) was dissolved in a 1:1 mixture of AcOH/Ac₂O (4.5 mL), and the reaction mixture was stirred at 90 °C for 2 h. After evaporation in vacuo the crude residue was purified by flash chromatography (cyclohexane/ethyl acetate 7:3) to give the target compound as a yellow solid (36 mg, 99%). ¹H NMR (400 MHz, CDCl₃): δ 9.51 (d, 1H), 8.20 (d, 1H), 8.08 (dd, 1H), 7.92 (d, 1H), 7.93 (s, 3H), 7.60 (d, 1H), 7.41 (d, 1H), 7.14 (d, 1H), 2.60 (s, 3H), 2.42 (s, 3H). MS (*m/z*): 509.2 [MH]⁺.

3-[2,4-Bis(trifluoromethyl)phenyl]-5-methyl-7-[3-(1,3-thiazol-2-yl)-1H-pyrazol-1-yl]-2-(trifluoromethyl)-3H-imidazo[4,5-*b*]pyridine (44). Compound **62** (18 mg, 0.043 mmol) was dissolved in a 1:1 mixture of CF₃COOH/(CF₃CO)₂O (2 mL), and the reaction mixture was heated at reflux for 2 h. Then, an additional portion of (CF₃CO)₂O (1 mL) was added and the mixture was refluxed for 1 h. The solvent was evaporated in vacuo and the crude residue was purified by flash chromatography (cyclohexane/ethyl acetate 7:3) to give the target compound as a yellow solid (21 mg, 100%). ¹H NMR (300 MHz, CDCl₃): δ 9.51 (d, 1H), 8.08 (s, 1H), 7.95 (d, 1H), 7.89 (d, 2H), 7.65 (d, 2H), 7.43 (d, 1H), 7.19 (d, 1H), 2.69 (s, 3H). MS (*m/z*): 495.2 [MH]⁺.

2-Chloro-3-([(1,1-dimethylethyl)(dimethyl)silyloxy)methyl]-6-methyl-4-[3-(1,3-thiazol-2-yl)-1H-pyrazol-1-yl]pyridine (63). To a solution of **49** (262 mg, 0.82 mmol) in DMF (10 mL) were added at room temperature *tert*-butyldimethylsilyl chloride (361 mg, 2.4 mmol), imidazole (644 mg, 9.46 mmol), and a catalytic amount of *N,N*-dimethylaminopyridine. The resulting reaction mixture was

stirred at room temperature for 12 h. Then, the solvent was removed in vacuo and the residue was partitioned between saturated aqueous NH_4Cl and ethyl acetate. The organic layer was separated, dried (Na_2SO_4), filtered, and concentrated in vacuo. The crude residue was purified by flash chromatography (cyclohexane/ethyl acetate 8:2) to give the target compound (295 mg, 85%). ^1H NMR (400 MHz, CDCl_3): δ 8.16 (d, 1H), 7.72 (d, 1H), 7.31 (s, 1H), 7.18 (d, 1H), 6.89 (d, 1H), 4.57 (s, 2H), 2.42 (s, 3H), 0.76 (s, 9H), 0.00 (s, 6H). MS (m/z): 421.5 $[\text{M}]^+$.

N-[2,4-Bis(trifluoromethyl)phenyl]-3-((1,1-dimethylethyl)(dimethyl)silyloxy)methyl)-6-methyl-4-[3-(1,3-thiazol-2-yl)-1H-pyrazol-1-yl]-2-pyridinamine (64). In a microwave vial were mixed at room temperature $\text{Pd}_2(\text{dba})_3$ (33 mg, 0.036 mmol), 2-(dicyclohexylphosphino)-2'-methylbiphenyl (40 mg, 0.108 mmol), K_3PO_4 (206 mg, 0.972 mmol), 2,4-bis(trifluoromethyl)aniline (164 mg, 0.71 mmol), and intermediate **63** (97, 150 mg, 0.36 mmol) in dry DME (1 mL). The vial was sealed and irradiated twice in a microwave apparatus for 20 min (80 W, 100 °C, 26 psi). The reaction mixture was then cooled to room temperature and quenched with saturated aqueous NH_4Cl . The aqueous phase was extracted with ethyl acetate, and the combined extracts were dried (Na_2SO_4), filtered, and concentrated in vacuo. The crude product was purified by flash chromatography (cyclohexane/ethyl acetate 95:5) to give the target compound (91 mg, 41%). ^1H NMR (400 MHz, CDCl_3): δ 8.58 (s, 1H), 8.51 (d, 1H), 7.93 (d, 1H), 7.87 (s, 1H), 7.79 (d, 1H), 7.78 (d, 1H), 7.40 (d, 1H), 7.13 (d, 1H), 6.90 (s, 1H), 4.95 (s, 2H), 2.56 (s, 3H), 0.84 (s, 9H), 0.03 (s, 6H). MS (m/z): 614.3 $[\text{MH}]^+$.

(2-([2,4-Bis(trifluoromethyl)phenyl]amino)-6-methyl-4-[3-(1,3-thiazol-2-yl)-1H-pyrazol-1-yl]-3-pyridinyl)methanol (65). To a solution of intermediate **64** (90 mg, 0.15 mmol) in THF (3 mL), at room temperature, was added TEA \cdot 3HF (1.5 mL, 2.22 mmol), and the resulting reaction mixture was stirred for 15 h. Saturated aqueous NH_4Cl was then added and extracted with ethyl acetate. The combined organic extracts were dried (Na_2SO_4), filtered, and concentrated in vacuo. The crude residue was purified by flash chromatography (cyclohexane/ethyl acetate 8:2) to give the target compound (36 mg, 50%). ^1H NMR (400 MHz, CDCl_3): δ 8.67 (d, 1H), 8.18 (s, 1H), 7.88 (m, 2H), 7.67 (d, 1H), 7.33 (d, 1H), 7.02 (d, 1H), 6.90 (s, 1H), 4.71 (d, 2H), 3.05 (t, 1H), 2.49 (s, 3H). MS (m/z): 500.2 $[\text{MH}]^+$.

N-[2,4-Bis(trifluoromethyl)phenyl]-3-(chloromethyl)-6-methyl-4-[3-(1,3-thiazol-2-yl)-1H-pyrazol-1-yl]-2-pyridinamine (66). To a solution of intermediate **65** (40 mg, 0.08 mmol) in dichloromethane (5 mL), at room temperature, SOCl_2 was added in large excess (0.2 mL, 3 mmol). The resulting solution was then heated at 40 °C for 1 h. The reaction mixture was then quenched with saturated aqueous Na_2CO_3 and extracted with dichloromethane. The combined organic extracts were dried (Na_2SO_4), filtered, and concentrated in vacuo. The crude product was purified by flash chromatography (cyclohexane/ethyl acetate 8:2) to give the target compound (32 mg, 78%). ^1H NMR (400 MHz, CDCl_3): δ 8.45 (d, 1H), 8.01 (s, 1H), 7.89 (m, 2H), 7.78 (d, 1H), 7.55 (s, 1H), 7.38 (d, 1H), 7.14 (d, 1H), 7.04 (s, 1H), 4.72 (d, 2H), 2.54 (s, 3H). MS (m/z): 518.2 $[\text{MH}]^+$.

(2-([2,4-Bis(trifluoromethyl)phenyl]amino)-6-methyl-4-[3-(1,3-thiazol-2-yl)-1H-pyrazol-1-yl]-3-pyridinyl)methanesulfonic Sodium Salt (67). To a solution of intermediate **66** (38 mg, 0.06 mmol) in CH_3CN (2 mL) was added Na_2SO_3 (42 mg, 0.32 mmol) dissolved in 4 mL of H_2O , and the resulting reaction mixture was stirred at room temperature for 15 min. The solvent was then evaporated in vacuo and the resulting crude material purified by flash chromatography (ethyl acetate/methanol 95:5) to give the target compound (33 mg, 100%). ^1H NMR (300 MHz, CDCl_3): δ 9.99 (s, 1H), 9.10 (s, 1H), 7.91 (d, 1H), 7.75–7.90 (m, 4H), 7.67 (d, 1H), 7.16 (s, 1H), 7.03 (d, 1H), 3.85 (s, 2H), 2.46 (s, 3H). MS (m/z): 564.2 $[\text{MH}]^+$.

1-[2,4-Bis(trifluoromethyl)phenyl]-6-methyl-4-[3-(1,3-thiazol-2-yl)-1H-pyrazol-1-yl]-1,3-dihydroisothiazolo[3,4-*b*]pyridine 2,2-Dioxide (45). A suspension of intermediate **67** (33 mg, 0.06 mmol) in distilled POCl_3 (1 mL) was heated at 170 °C in a Sure/Seal vial for 20 min. The reaction mixture was cooled to room temperature

and poured slowly into cold water. Saturated aqueous NaHCO_3 was slowly added until neutrality was attained. Ethyl acetate was added and the organic layer separated and the aqueous layer extracted with ethyl acetate. The combined organic extracts were dried (Na_2SO_4), filtered, and concentrated in vacuo. The crude black residue was purified by column chromatography (cyclohexane/ethyl acetate 5:4) to give the target compound (14 mg, 49%). ^1H NMR (400 MHz, CDCl_3): δ 8.11 (d, 1H), 8.10 (s, 1H), 8.00 (dd, 1H), 7.92 (d, 1H), 7.80 (d, 1H), 7.43 (d, 1H), 7.14 (d, 1H), 6.96 (s, 1H), 5.0–5.3 (dd, 2H), 2.41 (s, 3H). MS (m/z): 546.5 $[\text{MH}]^+$.

2,4-Dichloro-6-methylpyridine (69). To a solution of 4-hydroxy-6-methyl-2H-pyran-2-one **68** (10 g, 0.079 mol) in ethanol (24 mL) in a screw-cap vial was added a 28% aqueous NH_4OH (11 mL), and the reaction mixture was heated at 130 °C for 24 h. The solvent was then removed in vacuo, and the residue was used without any further purification. This crude material (5 g, 0.04 mol) and POCl_3 (24 mg, 0.16 mol) were heated at 120 °C in a screw-cap vial for 36 h. The reaction mixture was then cooled at ambient temperature and poured into crushed ice. Then, saturated aqueous NaHCO_3 was added until pH 8 was attained. Ethyl acetate was added and the organic layer separated, washed with brine, dried (Na_2SO_4), and concentrated in vacuo. The crude residue was purified by flash chromatography (cyclohexane/ethyl acetate 95:5) to give the title compound (5.18 g, 81%). ^1H NMR (400 MHz, CDCl_3): δ 7.40 (s, 1H), 7.18 (s, 1H), 2.71 (s, 3H). MS (m/z): 234.2 $[\text{MH}]^+$.

2-Chloro-6-methyl-4-[3-(1,3-thiazol-2-yl)-1H-pyrazol-1-yl]pyridine (70). To a solution of 2-(1H-pyrazol-3-yl)-1,3-thiazole (90 mg, 0.656 mmol) in dry DMF (1.5 mL) was added NaH (80% in mineral oil, 20 mg, 1.05 equiv) at 0 °C, and the reaction mixture was stirred for 20 min at room temperature. A solution of intermediate **69** (100 mg, 0.625 mmol) in dry DMF was then added, and the resulting reaction mixture was stirred at 100 °C for 2.5 h. The reaction was then quenched with water. The aqueous layer was extracted with ethyl acetate, and the organic layer was washed with brine, dried (Na_2SO_4), and concentrated in vacuo. The crude residue was purified by flash chromatography (ethyl acetate/cyclohexane 3:7) to give the desired compound (92 mg, 53%). ^1H NMR (400 MHz, CDCl_3): δ 8.06 (d, 1H), 7.92 (d, 1H), 7.59 (d, 1H), 7.52 (d, 1H), 7.41 (d, 1H), 7.12 (d, 1H), 2.63 (s, 3H). MS (m/z): 234.2 $[\text{MH}]^+$.

5-(Methyloxy)-1-(6-methyl-4-[3-(1,3-thiazol-2-yl)-1H-pyrazol-1-yl]-2-pyridinyl)-2,3-dihydro-1H-indole (46). $\text{Pd}_2(\text{dba})_3$ (10 mg, 0.011 mmol), dicyclohexyl(2'-methyl-2-biphenyl)phosphane (12 mg, 0.032 mmol), K_3PO_4 (64 mg, 0.3 mmol), compound **70** (103, 30 mg, 0.108 mmol), and 5-(methyloxy)-2,3-dihydro-1H-indole **71** (104, 32 mg, 0.216 mmol) were dissolved in dry DME (1 mL). The vial was sealed and irradiated in a microwave apparatus for 10 min (150 W, 100 °C, 60 psi, 8 cycles). The reaction mixture was then cooled to room temperature and quenched with saturated NH_4Cl . Ethyl acetate was added, and the organic layer was separated, washed with brine, dried (Na_2SO_4), and concentrated in vacuo. The crude residue was then purified by flash chromatography (cyclohexane/ethyl acetate 7:3) to give the title compound (8 mg, 19%). ^1H NMR (400 MHz, CDCl_3): δ 8.40 (d, 1H), 8.02 (m, 1H), 7.91 (m, 1H), 7.48 (d, 1H), 7.37 (d, 1H), 7.04 (d, 1H), 6.89 (d, 1H), 6.71 (m, 2H), 4.11 (t, 2H), 3.79 (s, 3H), 3.17 (t, 2H), 2.46 (s, 3H). MS (m/z): 390.2 $[\text{MH}]^+$.

In Vitro Biology. The CRF1 receptor-binding assay uses the homogeneous technique of scintillation proximity (SPA). The ligand (^{125}I]suvagine) binds to CRF1 receptor present in membranes prepared from recombinant CHO cells, which in turn bind to wheat germ agglutinin coated SPA beads. The signal generated is measured as CPM and is directly proportional to the amount of ligand bound to the receptor.

The ^{125}I]suvagine SPA is performed in a final volume of 100 μL using Costar white, clear-bottomed, 96-well plates, 5 μL of drug solution in neat DMSO, and 95 μL of a mixture of PVT WGA beads (1.0 mg/well), CRF1-CHO cell membranes (20 μg /well), and ^{125}I]suvagine (0.025 nM) in 50 mM HEPES/KOH, pH 7.40, 2 mM EDTA, 10 mM MgCl_2 . All values in parentheses are final assay concentrations. The nonspecific binding is measured in the presence of 1 μM unlabeled CRF. After addition of all reagents, plates were

shaken gently for 15 min, incubated overnight at room temperature, and read the following day using a Perkin-Elmer Trilux 1 min counting time per well.

Acknowledgment. The authors thank the colleagues who helped to generate all the data reported in this manuscript. In particular, a special thanks is due to the entire Verona NMR group for the NMR spectra and to Dr. Mahmoud Hamdan and his group for the mass spectra.

Supporting Information Available: Table of in silico properties of various compounds. This material is available free of charge via the Internet at <http://pubs.acs.org>.

References

- Holsboer, F. The rationale for corticotropin-releasing hormone receptors (CRH-R) antagonists to treat depression and anxiety. *J. Psychiatr. Res.* **1999**, *33*, 181–214.
- Vale, W.; Spiess, J.; Rivier, C.; Rivier, J. Characterization of a 41-residue ovine hypothalamic peptide that stimulates secretion of corticotropin and beta-endorphin. *Science* **1981**, *213*, 1394–1397.
- De Souza, E. B.; Nemeroff, C. B. *Corticotropin-Releasing Factor, Basic and Clinical Studies of a Neuropeptide*; CRC Press, Inc.: Boca Raton, FL, 1990.
- Dunn, A. J.; Berridge, C. W. Physiological and behavioural response to corticotropin-releasing factor administration: is CRF a mediator of anxiety or stress responses? *Brain Res. Rev.* **1990**, *15*, 71–100.
- Owen, M. J.; Nemeroff, C. B. Physiology and pharmacology of corticotropin-releasing factor. *Pharmacol. Res.* **1991**, *43*, 425–473.
- De Souza, E. B. Corticotropin-releasing factor receptors: physiology, pharmacology, biochemistry and role in central nervous system and immune disorders. *Psychoneuroendocrinology* **1995**, *20*, 789–819.
- Rivier, C.; Vale, W. Modulation of stress-induced ATCH release by corticotropin-releasing factor, catecholamines and vasopressin. *Nature* **1983**, *305*, 325–327.
- Raubenheimer, P. J.; Young, E. A.; Andrew, R.; Secki, J. R. The role of corticosterone in human hypothalamic–pituitary–adrenal axis feedback. *Clin. Endocrinol.* **2006**, *65*, 22–26.
- Holsboer, F.; Von Gardelen, U.; Gerken, A.; Stalla, G. K.; Muller, O. A. Blunted corticotropin and normal cortisol response in human corticotropin-releasing factor in depression. *N. Engl. J. Med.* **1984**, *311*, 1127.
- Kluge, M.; Schussler, P.; Kunzel, H. E.; Dresler, M.; Yassouridis, A.; Steiger, A. Increased nocturnal secretion of ACTH and cortisol in obsessive compulsive disorder. *J. Psychiatr. Res.* **2007**, *41*, 928–933.
- Chalmers, D. T.; Lovemberg, T. W.; Grigoriadis, D. E.; Behan, D. P.; De Souza, E. B. Corticotropin releasing-factor receptors: from molecular biology to drug design. *Trends Pharmacol. Sci.* **1996**, *17*, 166.
- Nemeroff, C. B.; Owens, M. J.; Bissette, G.; Andorn, A. C.; Stanley, M. Reduced corticotropin releasing factor binding sites in the frontal cortex of suicide victims. *Arch. Gen. Psychiatry* **1988**, *45*, 577–579.
- Banki, C. M.; Bissette, G.; Arato, M.; O'Connor, L.; Nemeroff, C. B. CSF corticotropin-releasing factor-like immunoreactivity in depression and schizophrenia. *Am. J. Psychiatry* **1987**, *144*, 873–877.
- De Bellis, M. D.; Gold, P. W.; Geraciotti, T. D., Jr.; Listwak, S. J.; Kling, M. A. Association of fluoxetine treatment with reductions in CSF concentrations of corticotropin-releasing hormone and arginine vasopressin in patients with major depression. *Am. J. Psychiatry* **1993**, *150*, 656–657.
- Raadsheer, F. C.; van Heerikhuizen, J. J.; Lucassen, P. J.; Hoogendijk, W. J.; Tilders, F. J.; Swaab, D. F. Corticotropin-releasing hormone mRNA levels in the paraventricular nucleus of patients with Alzheimer's disease and depression. *Am. J. Psychiatry* **1995**, *152*, 1372–1376.
- Nemeroff, C. B.; Bissette, G.; Akil, H.; Fink, M. Neuropeptide concentrations in the cerebrospinal fluid of depressed patients treated with electroconvulsive therapy. Corticotropin-releasing factor, beta-endorphin and somatostatin. *Br. J. Psychiatry* **1991**, *158*, 59–63.
- Zobel, A. W.; Nickel, T.; Kunzel, H. E.; Ackl, N.; Sonntag, A.; Ising, M.; Holsboer, F. Effects of the high-affinity corticotropin-releasing hormone receptor 1 antagonist R121919 in major depression: the first 20 patients treated. *J. Psychiatr. Res.* **2000**, *34*, 171–181.
- Chen, C. Recent advances in small molecule antagonists of the corticotropin-releasing factor of type-1 receptor. Focus on pharmacology and pharmacokinetics. *Curr. Med. Chem.* **2006**, *13*, 1261–1282, and references cited therein.
- Arban, R.; Benedetti, R.; Bonanomi, G.; Capelli, A. M.; Castiglioni, E.; Contini, S.; Degiorgis, F.; Di Felice, P.; Donati, D.; Fazzolari, E.; Gentile, G.; Marchionni, C.; Marchioro, C.; Messina, F.; Micheli, F.; Oliosi, B.; Pavone, F.; Pasquarello, A.; Perini, B.; Rinaldi, M.; Sabbatini, F. M.; Vitulli, G.; Zaranonello, P.; Di Fabio, R.; St-Denis, Y. Cyclopenta[d]pyrimidines and dihydropyrrolo[2,3-d]pyrimidines as potent and selective corticotropin-releasing factor 1 receptor antagonists. *ChemMedChem* **2007**, *2*, 528–540.
- Sabbatini, F. M.; Di Fabio, R.; St-Denis, Y.; Capelli, A. M.; Castiglioni, E.; Contini, S.; Daniele, D.; Fazzolari, E.; Gentile, G.; Micheli, F.; Pavone, F.; Rinaldi, M.; Pasquarello, A.; Zampori, M. G.; Di Felice, P.; Zaranonello, P.; Arban, R.; Perini, B.; Vitulli, G.; Benedetti, R.; Oliosi, B.; Worby, A. Heteroaryl substituted 4-(1H-pyrazol-1-yl)-5,6-dihydro-1H-pyrrolo[2,3-d]pyrimidine derivatives as potent and selective corticotropin-releasing factor receptor-1 antagonists. *ChemMedChem* **2008**, *3*, 226–229.
- For an alternative series of CRF-1 receptor antagonists, see the following article: Gentile, G.; Di Fabio, R.; Pavone, F.; Sabbatini, F. M.; St-Denis, Y.; Zampori, M. G.; Vitulli, G.; Worby, A. Novel substituted tetrahydrotriazacene derivatives as potent CRF1 receptor antagonists. *Bioorg. Med. Chem. Lett.* **2007**, *17*, 5218–5221.
- Mittelbach, M. An easy and convenient synthesis of 6-methyl-4(1H)-pyridone-3-carboxylic acid. *Synthesis* **1988**, *6*, 479–480.
- Dunn, W. J., III. Quantitative structure–activity relationship. *Chemom. Intell. Lab. Syst.* **1989**, *6*, 181–190.
- Miyashita, Y.; Ohsako, H.; Takayama, C.; Sasaki, S. Multivariate structure–activity relationships analysis of fungicidal and herbicidal thiocarbamates using partial least squares method. *Quant. Struct.–Act. Relat.* **1992**, *11*, 17–22.
- Hasegawa, K.; Miyashita, Y.; Sasaki, S.-I.; Sonoki, H.; Shigyou, H. Quantitative structure–activity relationship study of antiarrhythmic phenylpyridines using multivariate partial least squares modelling. *Chemom. Intell. Lab. Syst.* **1992**, *16*, 69–75.
- Geladi, P.; Kowalski, B. R. An example of 2-block predictive partial least-squares regression with simulated data. *Anal. Chim. Acta* **1986**, *185*, 19–32.
- Hoskludsson, A. J. *Chemometrics* **1988**, *2*, 221.
- Glen, W. G. *Tetrahedron Comput. Methodol.* **1989**, *2*, 349.
- Hansch, C.; Leo, A.; Unger, S. H.; Kim, K. H.; Nikaitani, D.; Lien, E. J. "Aromatic" substituent constants for structure–activity correlations. *J. Med. Chem.* **1973**, *16*, 1207–1216.
- SIMCA-P+11.5*; Umetrics AB: Umeå, Sweden.
- Eastment, H.; Krzanowski, W. Crossvalidatory choice of the number of components from a principal component analysis. *Technometrics* **1982**, *24*, 73–77.
- Palczewski, K.; Kumasaka, T.; Hori, T.; Behnke, C. A.; Motoshima, H.; Fox, B. A.; Le Trong, I.; Teller, D. C.; Okada, T.; Stenkamp, R. E.; Yamamoto, M.; Miyano, M. Crystal structure of rhodopsin: a G protein-coupled receptor. *Science* **2000**, *289*, 739–745.
- Donnelly, D.; Overington, J. P.; Blundell, T. L. The prediction and orientation of α -helices from sequence alignments: the combined use of environment-dependent substitution tables, Fourier transform methods and helix capping rules. *Protein Eng.* **1994**, *7*, 645–653.
- Brooks, B. R.; Brucoleri, R. E.; Olafson, B. D.; States, D. J.; Swaminathan, S.; Karplus, M. CHARMM: a program for macromolecular energy, minimization, and dynamics calculations. *J. Comput. Chem.* **1983**, *4*, 187–217.
- Dunbrack, R. L., Jr.; Karplus, M. Backbone-dependent rotamer library for proteins. Application to side-chain prediction. *J. Mol. Biol.* **1993**, *230*, 543–574.
- Batchmin*, version 8.5; Schrodinger LLC: Portland, OR.
- Chen, R.; Lewis, K. A.; Perrin, M. H.; Vale, W. Expression cloning of a human corticotropin-releasing-factor receptor. *Proc. Natl. Acad. Sci. U.S.A.* **1993**, *90*, 8967–8971.
- Liaw, C. W.; Grigoriadis, D. E.; Lovemberg, T. W.; De Souza, E. B.; Maki, R. A. Localization of ligand-binding domains of human corticotropin-releasing factor receptor: a chimeric receptor approach. *Mol. Endocrinol.* **1997**, *11*, 980–985.

JM800743Q